ANNEXIN A2 IS REQUIRED FOR ENDOTHELIAL CELL JUNCTIONAL RESPONSE TO S1P

A Thesis

by

REBECCA LYNN SMITH

Submitted to the Office of Graduate and Professional Studies of
Texas A&M University
in partial fulfillment of the requirements for the degree of

MASTER OF SCIENCE

Chair of Committee,	Kayla Bayless
Committee Members,	Roland Kaunas
	Emily Wilson
Head of Department,	Geoffrey Kapler

May 2014

Major Subject: Medical Sciences

ABSTRACT

Endothelial cell (EC) junctions are critical for angiogenesis, the sprouting and growth of new blood vessels from existing vessels. Sphingosine 1-phosphate (S1P) is a proangiogenic factor that potently stimulates sprouting, fortifies EC junctions, and work by others has shown it stimulates VE-cadherin, α-catenin, focal adhesion kinase (FAK) and paxillin junction localization among others. Annexin A2 (ANXA2), a calcium-regulated membrane-binding and adapter protein, has a known role in angiogenesis. Previously, we showed that ANXA2 is required for barrier integrity by binding to vascular endothelial (VE)-Cadherin and preventing its phosphorylation. Thus, we tested whether ANXA2 silencing in human endothelial cells alters localization of junctional and focal adhesion proteins with immunofluorescence staining.

Removal of the ANXA2 protein in ECs resulted in the formation of wide reticular junctions in 2D, affecting localization of adherens junction proteins such as VE-cadherin, platelet endothelial cell adhesion molecule-1 (PECAM-1), filamin A, and α- and β-catenin. Additionally, when ANXA2 was silenced, neither FAK, paxillin, nor vinculin formed large focal adhesions near the cell-cell junctions, particularly, near the reticular cell-cell junctions. Reticular junctions were reported in the literature in non-transduced cells seeded on fibronectin coated glass coverslips. We showed that these reticular junctions were present in ECs seeded on collagen I-, collagen IV-, and Matrigel-coated glass coverslips in addition to fibronectin. We characterized these reticular junctions temporally, showing the number of reticular junctions increased over

time, particularly after 8 hours in low serum culture medium. Levels of VE-cadherin and zonula occludens-1 (ZO-1) were also regulated over time in cells forming reticular junctions, upregulated at 4 hours and 12 hours, respectively.

Most striking was the affect S1P had on reticular junction formation. The addition of S1P to ECs abrogated the formation of reticular junctions in 2D. Upon comparison of the proteins involved, the shANXA2 reticular junctions and the non-transduced EC reticular junctions appeared similar. In both groups only adherens junctions proteins participated in reticular localization while focal adhesion proteins and tight junction proteins did not localize in a reticular pattern. The junctions differed, however, in that the shANXA2 reticular junctions formed in the presence of S1P while the non-transduced reticular junctions did not, indicating ANXA2 is required for proper junctional response to S1P. Finally, we show the presence of reticular junctions in EC monolayers on 3D collagen matrices, reticular junctions contributing to EC sprout initiation, and reticular junctions present in mouse uterine tissue from pregnant mice 7.5 days after implantation. The discoveries detailed in this thesis illustrate the importance of ANXA2 in EC junctional response to S1P as well as the potential for future discoveries concerning the role of reticular junctions in sprouting angiogenesis.

DEDICATION

For my loving husband, Ben, who has been by my side, supporting me every step of the way, and for the glory of the Lord, Jesus Christ whose love is never-failing.

ACKNOWLEDGEMENTS

To all who made this work possible, I thank you. Specifically, I would like to thank my committee chair, Dr. Kayla Bayless for her continued encouragement and guidance, as well as my committee members, Drs. Roland Kaunas and Emily Wilson, for their support.

A special thanks to the Biomedical Engineering department at Texas A&M University for their help quantifying focal adhesions, in particular Dr. Po Feng Lee. Additionally, I would like to thank Drs. Bryan White and Heewon Seo for their help in obtaining, sectioning, and staining the mouse uterine tissue samples.

I would also like to thank all of my colleagues, friends, faculty and members of the Department of Molecular and Cellular Medicine who helped make my time here enjoyable and fruitful. Specifically, the members of the Bayless Lab have proved invaluable. Colette Abbey, Dr. Hojin Kang, Dr. David Howell, Jui Dave, and Camille Duran, thank you for your constant support, occasional help with experiments, and always encouraging criticism.

Finally, I would like to thank my family, whose love and encouragement prompted me to extend my education and kept me sane throughout the journey.

NOMENCLATURE

EC	Endothelial Cell
S1P	Sphingosine 1-phosphate
FAK	Focal Adhesion Kinase
VE-Cadherin	Vascular Endothelial-Cadherin
ANXA2	Annexin A2
PECAM-1	Platelet Endothelial Cell Adhesion Molecule-1
ZO-1	Zonula Occludens-1
MMP	Matrix Metalloproteinases
VEGF	Vascular Endothelial Growth Factor
bFGF	Basic Fibroblast Growth Factor
GPCR	G-protein Coupled Receptors
AJ	Adherens Junction
TJ	Tight Junction

TABLE OF CONTENTS

Page

LIST OF FIGURES

Page

CHAPTER I

INTRODUCTION AND LITERATURE REVIEW

Introduction to Angiogenesis

Blood vessel growth and maintenance is a rapid and dynamic process. There are several known modes of blood vessel growth. Vasculogenesis is the assembly of neovessels from precursor cells that differentiate into endothelial cells (ECs) and is required for early vascular development (1; 2); intussusception is a type of vessel splitting potentially important during skeletal muscle growth (3), pregnancy (4), and tumor growth (5); and sprouting angiogenesis is the outgrowth of a new vessel from an existing vessel during development, wound healing, and pathological events (6; 7). Each of these processes is dependent on physiological signals that work together to activate endothelial cells.

Angiogenesis is a multi-step process directed by growth factors, lipids, and mechanical stimuli in the bloodstream and surrounding tissues (8; 9). Angiogenesis is initiated when proangiogenic stimuli activate endothelial receptors, such as G-protein coupled receptors and tyrosine kinase receptors, and mechanosensors, such as integrins and junctional complexes, on the EC surface (10; 11). In response to the signal, ECs are activated resulting in a change in gene expression known as the "angiogenic switch" (12). Additionally, the vascular permeability of the EC barrier is altered (13; 14). Sprout formation occurs following tip and stalk cell determination by the Dll4 and Notch pathway (15). As the sprout forms, matrix metalloproteinases (MMPs) anchored to the

EC membrane (16; 17), begin to degrade the surrounding basement membrane and surrounding extracellular matrix to provide a tunnel for EC migration (18-20). Following outgrowth, the neovessel matures by creating an inner lumen for blood flow (21), and the ECs begin to remodel the surrounding extracellular matrix by recruiting pericytes and other supportive cells to generate and deposit collagen IV-rich basement membrane (22).

In healthy, quiescent or non-activated vessels, levels of factors that stimulate EC sprouting are typically very low, and as a result, ECs attach to each other via cell-cell junctions and form a single, continuous, and thin monolayer. These junctions are key to blood vessel health and vital during angiogenesis, creating a selectively permeable barrier between the lumen of the vessel and the tissues surrounding the vessel (23). Vessel permeability is often altered during angiogenesis by a variety of factors, the balance of which determines the propensity of the vessel to begin branching (24-26). Growth factors increase vascular permeability of blood vessels by acting on junctional proteins, compromising the integrity of the barrier created by adjoining ECs (27; 28). Vascular endothelial growth factor (VEGF) and basic fibroblast growth factor (bFGF), are also known as vascular permeability factor (29) and tumor angiogenesis factor (30), respectively. VEGF and bFGF are upregulated during pregnancy and produced by tumor cells to increase vascular permeability and initiate directional blood vessel growth; both VEGF and bFGF are currently used in angiogenesis assays to stimulate EC sprouting (31; 32). Conversely, ~5 dynes/cm^2 fluid shear stress, which has been observed in post capillary venules, and sphingosine 1-phosphate (S1P), a platelet-derived bioactive lipid

found in the bloodstream reinforce cell-cell junctions (33-36). Because angiogenic cues modify EC junctions and sprout initiation depends so heavily on the presence of junctional molecules, in this study we explore in more detail the key signals that may regulate localization of various proteins to the EC junction in response to stimuli that trigger angiogenic sprouting, including S1P, growth factors, and shear stress.

Sphingosine 1-phosphate

S1P is generated by hydrolysis of membrane lipids in platelets activated during wound healing or other pathological events (32). It was first discovered as the primary barrier-protective product of platelets by Dudek and Garcia (37; 38). S1P binds to and activates the S1P1, S1P2, and S1P3 G protein-coupled receptors (GPCRs). Primary human umbilical vein ECs express S1P1 (EDG1) and S1P3 (EDG3) on their surface, but do not express S1P2 (EDG5) (39). The proangiogenic effects of S1P occur through S1P1 and S1P3, stimulating EC proliferation and survival, migration, and tube formation, (36; 40; 41). In particular, upon ligand binding to S1P1 or S1P3 the receptors transduce signals through the PI3K/Akt/Rac small GTPase pathway inducing changes in the cytoskeleton such as stress fiber and cortical actin formation (42; 43).

S1P also initiates angiogenesis by activating MMPs. In ECs, expression of MMP2 or gelatinase A, once thought to be the primary contributor to cell invasion due to its ability to degrade type I and type IV collagens (44; 45), is upregulated following S1P treatment (46). More recent studies have shown that the membrane bound MMPs, particularly MT1-MMP, are the primary MMPs required for EC invasion (47-49). MT1-

MMP is activated by S1P via phosphorylation of tyrosine 573 on its cytoplasmic tail and translocation of the protein to the plasma membrane (16; 17; 50; 51). This activation initiates 3D cell invasion via matrix degradation as well as the activation of other MMPs, such as MMP2, downstream of MT1-MMP (48; 52; 53).

Finally, and most importantly for this study, S1P stimulates angiogenesis through barrier enhancement. S1P induces a rise in intracellular calcium that promotes cell spreading and barrier stability through Rac activation and adherens junction assembly (54-56). While VEGF causes barrier destabilization to initiate angiogenesis (28), S1P is required during angiogenesis to stabilize focal adhesions (57), cell-cell junctions (36), the interactions between cell junctions and focal adhesions via the cortical actin ring (58), and initiate restabilization of the neovessel through EC recruitment of pericytes and smooth muscle cells that support the new vasculature (59). The following sections illustrate specific types of junctions observed in ECs.

Cell Junctions: Adherens Junctions

ECs bind to each other via several types of junctions – adherens junctions, tight junctions, and gap junctions – that each provides different functions to the monolayer. In ECs the three types of junctions are intermingled between the apical and basal (facing the extracellular matrix) side of the cell (60; 61). The adherens junctions provide mechanical strength to the endothelial barrier and allow the transmittance of mechanical signals to neighboring cells; the tight junctions prevent the flow of fluid or solutes between the cells by tightly binding the cells together; and the gap junctions provide a

continuous signaling linkage between cells to transfer chemical or electrical signals almost instantaneously (62; 63). Each junction contains specialized proteins that respond differently to angiogenic signals.

In this study we will focus mainly on the adherens and tight junctions (AJs and TJs respectively). The main components of the endothelial AJs, vascular endothelial (VE)-cadherin and platelet endothelial cell adhesion molecule-1 (PECAM-1/CD31) are stabilized by intracellular catenins and other junctional proteins (62; 64). VE-cadherin and PECAM-1 are cell adhesion molecules or CAMs exhibiting single-pass transmembrane glycoproteins that promote homophilic binding and adhesion between cells under quiescent conditions (65-67). While the removal of either VE-cadherin (68) or PECAM-1 (unpublished data) from ECs inhibits EC sprouting, the functions of the individual proteins and responses to angiogenic stimuli are unique and are detailed in the following paragraphs.

VE-cadherin readily associates with intracellular junction-stabilizing proteins such as p120 catenin, β-catenin, and plakoglobin (γ-catenin) among others to comprise the AJ (69). The p120 catenin promotes strong cell-cell adhesion by stabilizing VE-cadherin to the plasma membrane and controlling VE-cadherin clustering (70). VE-cadherin is often assumed to connect to the actin cytoskeleton through the interaction of α-catenin (which can bind to β-catenin and plakoglobin) with actin; however, this has been disputed by Nelson and colleagues, who showed that α-catenin does not interact with actin filaments and the β-catenin/VE-cadherin complex simultaneously (71). Another possible interaction of the AJ and the cell cytoskeleton is the association

between VE-cadherin, plakoglobin, desmoplakin, and vimentin (72). The phosphorylation status of each of these proteins and cadherins changes the strength of adhesion between the neighboring cells. In general, an increase in phosphorylation of VE-cadherin and the catenins decreases the adhesive strength of the junction (73). During angiogenesis, the adhesion between cells is manipulated via the phosphorylation and relocation of VE-cadherin to promote migration and cell sprouting. VEGF has been shown to increase the tyrosine phosphorylation of VE-cadherin, p120 catenin, and β-catenin in HUVECs (74). VEGF-A (an isoform of VEGF) phosphorylates VEGFR2 (a VEGF receptor present on ECs) and stimulates VEGFR2 association with a Src family protein, which then phosphorylates VE-cadherin. This triggers endocytosis of the entire complex disrupting the adherens junction (70; 75; 76). This disruption is part of the angiogenic switch that causes the cells to give up a quiescent state in favor of a leaky and sprouting vasculature (70).

S1P has the opposite effect of VEGF on VE-cadherin. Hla and colleagues showed that S1P treatment induces AJ assembly in HUVECs (36). When HUVECs were treated with S1P, localization of VE-cadherin, α-, β-, and γ-catenin at cell-cell junctions was significantly increased within one hour in cultured ECs (36). Further, *in vivo* experiments illustrated that S1P is necessary for vessel maturation in growth factor induced angiogenesis, congruent with the hypothesis that, although VEGF and S1P have opposing effects on VE-cadherin, both are necessary for stable neovascularization (36).

Different from VE-cadherin, PECAM-1 is required to establish cell-cell contacts, but is not necessary to maintain them (77). Additionally, anti-huPECAM-1 antibody

treatments inhibited HUVEC tube formation and migration on Matrigel, an interaction that was independent of VE-cadherin but potentially could be compensated for with VE-cadherin (78). To illustrate the importance of PECAM-1 in endothelium establishment and maintenance, several studies addressed the responses of PECAM-1 to angiogenic stimuli, including phosphorylation and relocation.

PECAM-1 has several motifs in its cytoplasmic tail such as immunoreceptor tyrosine-based activation motif (ITAM) and immunoreceptor tyrosine-based inhibitory motif (ITIM). These motifs allow PECAM-1 to recruit and interact with adaptor molecules, such as those containing SH2 domains, to transmit extracellular signals into intracellular signals (79). In response to WSS, PECAM-1 acts as a mechanotransducer; the tyrosine sites of PECAM-1's cytoplasmic tail become phosphorylated, and recruit SHP-2, which induces cell survival and proliferation via extracellular-signal-related kinase ERK activation (80; 81). Fluid shear stress also initiates the complexing of PECAM-1, VE-cadherin, and VEGFR2 (81; 82). This complex activates the downstream PI3K and Akt pathways to promote angiogenesis. The effects of WSS on PECAM-1 show a function of PECAM-1 distinct from VE-cadherin, as only PECAM-1 can directly transmit mechanical force via phosphorylation of its cytoplasmic tail.

S1P also induces a migration-promoting response in ECs via PECAM-1 signaling. Madri and colleagues demonstrated that PECAM-1 was required for ECs to move as a group in a coordinated manner (i.e. wound healing migration) (83). Immortalized knock out mouse ECs lacking PECAM-1 exhibited single cell migration that was rescued using reconstituted full-length PECAM-1 (83). This mechanism was

Rho-mediated and inhibited by pertussis toxin, suggesting that it was Gαi-mediated. The knockout cells were not affected by S1P treatment, while HUVEC migration increased in response to S1P, indicating that PECAM-1 is required for the migratory response to S1P (83). Madri's group, among others, suggested that the interaction takes place between the cytoplasmic tail of PECAM-1 and the small G protein, Gαi2, which is important for signal transduction functions of the S1P receptors (79; 83).

Cell Junctions: Tight Junctions

While AJs proteins are required for vessel sprouting, TJ proteins are downregulated, suggesting that these junctions provide unique roles during angiogenesis (84). AJs provide structural integrity and the intertwined TJs ensure there is no leakage of fluid or molecules between the cells of the endothelium. The function of TJs is twofold: the barrier function creates a "seal" between adjacent ECs to prevent the flow of unwanted molecules into and out of the vasculature, and the fence function separates the apical and basolateral plasma membrane restricting the diffusion of lipids and proteins (85).

TJs are composed of three types of membrane proteins, and several associated peripheral membrane structural and regulatory proteins. Occludin, claudins, and junctional adhesion molecules (JAMs) are the main transmembrane components (86). Zonula occludens-1 (ZO-1) was the first of the main TJ-associated intracellular proteins identified that stabilized the EC junction (87), quickly followed by the discovery of claudins and occludin, the binding of which creates a seal between the cells (88). While

occludin is important for TJ regulation, claudins, specifically claudin-5, are the most critical proteins for TJ assembly in ECs (89; 90). As each of these proteins has different functions in TJs, they are each affected differently by angiogenic stimuli.

S1P has been shown to activate ZO-1 in HUVECs, causing it to translocate to lamellipodia and cell-cell junctions through an S1P1/Gi/Akt/Rac pathway, suggesting ZO-1 has a dual role in response to S1P, promoting migration and stabilizing TJs (91). ZO-1 interacts with cortactin, an actin-binding protein that redistributes to the leading edges of migratory cells and plays a role in S1P mediated chemotaxis (92). S1P induces cortactin and ZO-1 colocalization at lamellipodia, an effect attenuated by cortactin knockdown, suggesting that ZO-1/cortactin complexes regulate the EC's chemotactic response (91). Independent of cortactin, ZO-1 and α-catenin interact directly at cell-cell junctions suggesting the complex regulates endothelial barrier integrity (91; 93). Similar to its effect on VE-cadherin, S1P causes stabilization of tight junctions; however, it also affects the tendency of the cell to migrate by rearranging some of the tight junction proteins to migratory fronts and potentiating angiogenesis.

It is also shown that there is crosstalk between different types of junctions (94; 95). For example, VE-cadherin clustering at AJs, such as during S1P stimulation, upregulates the gene encoding Claudin-5, a tight junctional protein, by sequestering β-catenin. β-catenin, when not bound to VE-cadherin at the plasma membrane, is translocated to the nucleus where it prevents the phosphorylation (and inactivation) of the transcriptional Claudin-5 gene repressor, FoxO1 (96). Additionally, VE-cadherin clustering activates the PI3K-Akt pathway that initiates the phosphorylation of FoxO1

(95; 97) resulting in an increase of Claudin-5 production (95). These results demonstrate that S1P not only stabilizes AJs by securing VE-cadherin at cell-cell contacts, but also may strengthen TJs by upregulating the expression of Claudin-5.

Annexin Family of Proteins

The annexin family of proteins is comprised of calcium-regulated membrane binding proteins found in ECs among other cells types and named for "annex" because of their ability to aggregate proteins (98). Each of the annexin proteins contains four homologous domains of 5 alpha helices each. One or more of the domains contains the signature of the protein – the endonexin fold, calcium-binding motif (99). This study focuses primarily on Annexin A2 (ANXA2). ANXA2 is found in ECs, monocytes, macrophages, and most cancer cells, and can exist as a monomer or in a heterotetrameric complex with S100A10 (p11), a complex important for plasmin regulation (99). ANXA2 is unique among the annexins because it contains cysteine residues that are sensitive to reactive oxygen species (100). Surprisingly, ANXA2 null mice have a relatively benign phenotype considering the 61 genes that were found to be dysregulated in type-II alveolar cells depleted by short hairpin RNA targeting ANXA2 (99; 101).

ANXA2 is dysregulated in many cancers; invasive cancers such as ductal mammary carcinoma and pancreatic ductal adenocarcinoma, exhibit high levels of ANXA2 (99). One theory explaining this phenomenon suggests the increased amount of ANXA2 promotes the interaction of ANXA2 with p11 at the cell membrane causing a downstream increase of plasmin which is known to cleave MMPs from the pro form to

the active form (99). Additionally, ANXA1 and ANXA2 have been implicated in wound repair in epithelial cells. ANXA1 cleavage product, Ac2-26, was shown to initiate focal adhesion protein activation and cell migration via increased ROS production (102) and ANXA2 loss in epithelial cells resulted in inhibited migration and increased cell-matrix attachment via an increase in β1 integrin (103).

ANXA2 can function as a link between junctional proteins and the actin cytoskeleton, making it an ideal protein for monitoring the effects of S1P on interactions between cell-cell junctions and focal adhesions. Actin-rich AJs and TJs are mainly responsible for intercellular adhesion via the formation of actin filament associated protein complexes along transmembrane adhesion sites (60) and both require ANXA2 (104-106). ANXA2 was found to bind to F-actin and spectrin, recruit filamins A and B, and contribute to the reorganization of actin into cortical actin supporting barrier reinforcement (105-107). In response to S1P, our lab has shown that S1P stimulates ANXA2 translocation from the cell cytosol to the plasma membrane, where it complexes with VE-cadherin (108). When ANXA2 was depleted in ECs, Akt activation was attenuated resulting in increased phosphorylation of VE-cadherin, endothelial barrier leakage, and decreased EC invasion in 3D collagen matrices (108). These data indicate a key role for ANXA2 in regulating barrier function in ECs in response to S1P. One main goal of the studies described here is to better understand the role of ANXA2 in maintaining EC junctions and promoting successful endothelial sprouting.

Cell Junctions: Reticular Junctions

While much is known about the individual junctional proteins, their interactions with each other are constantly under investigation. Particularly, the most recent of these interactions coined "reticular junctions," is the least well known (109). Reticular junctions are found in quiescent EC monolayers where two ECs overlap (109). They are comprised of the junction surrounding PECAM-1 containing compartments collectively deemed the "subjunctional reticulum" (110). PECAM-1 is recycled to these compartments and can be rapidly accessed by the plasma membrane during leukocyte transendothelial migration (110). While PECAM-1 is found in the subjunctional compartments and the surrounding reticular region, VE-cadherin, α-, β-, and p120-catenin, only localize to the reticular region creating voids in a "honeycomb" staining pattern. ZO-1 and actin did not localize to the reticular region suggesting these may be regions of low tension (109). Importantly, these reticular junctions are seen in two distinct experiments performed in our laboratory. ANXA2 silencing results in increased formation of reticular junctions, and reticular junctions are observed in EC monolayers stimulated to invade 3D collagen matrices in response to S1P.

The long-term goal of our laboratory is to better understand the localization of junctional proteins in sprouting ECs that are stimulated to invade 3D collagen matrices in response to S1P and growth factors. Initially, we employed a 2D immunofluorescent model to better understand shANXA2 junctions, as well as, reticular junctions in a simple environment. Because ANXA2 binds to F-actin (105), it is required for the formation of actin-rich tight junctions (106), and reticular junctions lack actin

localization (109), we explored how the EC junctional proteins are localized when ANXA2 is silenced using shRNA. Interestingly, the silencing of ANXA2 in ECs resulted in a significant increase in the number of reticular junctions even at early time points. We characterize the reticular junctions in these cells as well as in non-transduced ECs with immunofluorescence illustrating a honeycomb distribution of VE-cadherin and catenins, and a disruption in focal adhesion stability. Following the observation of reticular junctions in shANXA2 cells and in non-transduced ECs, we explored the distribution of junctional proteins in reticular junctions temporally and following stimulation with the proangiogenic sphingolipid, S1P. The results show the presence of reticular junctions after at least 12 hours on several extracellular matrices. We also see a decrease in the number of reticular junctions in the presence of S1P on non-transduced ECs despite the formation of reticular junctions on shANXA2 cells in the presence of S1P. Finally, we observed the presence of reticular junctions in non-transduced ECs on 3D collagen matrices as well as sprout formation initiating from these junctions. We propose a novel model of how ECs invade from reticular junctions.

CHAPTER II

MATERIALS AND METHODS

Cell Culture

Human umbilical vein endothelial cells (ECs; Lonza; Cambridge, MA) were passaged weekly, and media were changed every four days. ECs were cultured on gelatin-coated (1mg/mL) T75 tissue culture flasks (Corning; Corning, NY) in growth medium containing Medium 199 (M199; Gibco; Carlsbad, CA), heparin (100μg/mL; Sigma-Aldrich; St. Louis, MO), 0.034% lyophilized endothelial growth supplement (Pel-Freeze Biologicals; Rogers, AR) prepared as described (111), 13% fetal bovine serum (FBS; Gibco; Carlsbad, CA), gentamycin (10μg/mL; Gibco; Carlsbad, CA), and antibiotics (Gibco; Carlsbad, CA) as described (112). All ECs were grown at 37^{o}C and 5% CO_2 and ECs used in all experiments were passage 3-6.

293FT cells (Invitrogen; Carlsbad, CA) were passaged every four days and cultured on collagen I-coated (20μg/mL) 100mm×20mm round tissue culture dishes (Corning; Corning, NY) in growth medium containing Dulbecco's Modified Eagle Medium (DMEM; Gibco; Carlsbad, CA), 10% fetal bovine serum (Gibco; Carlsbad, CA), 500 μg /mL G418 (Enzo Life Sciences; Farmingdale, NY), gentamycin (10μg/mL; Gibco; Carlsbad, CA), and antibiotics (Gibco; Carlsbad, CA) as described (112). 293FTs were grown at 37^{o}C and 5% CO_2 and were used in all experiments at passage 3-10.

Generation of Knockdown Cell Lines using shRNA

shRNA constructs were purchased from Sigma-Aldrich and prepared from glycerol stocks for annexin A2 (#SHCLNG-NM001002857; clones TRCN056144, shANXA2-1 and TRCN056145, shANXA2-2) and β_2-microglobulin (β2M; #SHCLNG-NM006098; clones TRCN057254, shβ2M-1 and TRCN057255, shβ2M-2). Lentiviral plasmid mixtures, containing 1.25μg of backbone shRNA lentiviral plasmid and 3.75μg of VIRAPOWER packaging mix (Invitrogen; Carlsbad, CA) were diluted separately in 500μL of Opti-MEM (Invitrogen; Carlsbad, CA) and combined with 12μL Lipofectamine 2000 (Invitrogen; Carlsbad, CA) in 500μL Opti-MEM after 5 minutes of incubation at room temperature. Lipofectamine mixtures were added to diluted DNA for 20 minutes. Meanwhile, 3×10^6 293FT cells (Invitrogen; Carlsbad, CA) were trypsinized, pelleted, and resuspended in 3mL of DMEM with 10% FBS. 1.5mL of cells and 1mL of transfection mixture were added to each T25. The media was changed 16 hours after transfection and viral supernatants were collected at 60 hours after transfection, centrifuged at 1000×g for 10 minutes and either frozen at -80^{o}C or used immediately to infect ECs.

For EC infection, 3×10^5 cells in 1mL of growth medium (to yield a confluency of 25-30%), 2mL viral supernatant, 2mL endothelial growth medium, and 12μg/mL Polybrene (Sigma-Aldrich; St. Louis, MO) were added to a gelatin coated T25 flask and allowed to incubate. Viral supernatants were removed and ECs were given fresh growth medium after 6 hours. Cells were allowed to grow for 4 days prior to use in experiments. ECs imaged under phase were rinsed with growth medium on day 4 and images were

taken at 4× magnification using an Olympus CKX41 microscope and a Q-Color 3 camera. Cells used in experiments were counted using a Nexcelom Cellometer Auto 1000 following trypsinization. Cell concentration and average cell diameter in microns were measured. Successful protein silencing was confirmed by Western blot analyses.

mRNA Extraction and RT-PCR Analysis

ECs were treated with shRNAs to annexin A2 and β2M. RNA was extracted from ECs expressing shRNA as well as an untreated control, using an RNeasy MiniKit (Qiagen; Valencia, CA). Eluted RNA was treated with RNase-free DNase (Qiagen; Valencia, CA) for 10 minutes at room temperature and inactivated at 65°C for 15 minutes. RNA quality was assessed by electrophoresis. cDNA was generated with the SuperScript III First-Strand Synthesis System (Invitrogen; Carlsbad, CA) using 1μg of RNA and Oligo(dT)20 following the manufacturer's instructions. The primers used for this study were: ANXA2 (NM_001002858.2; 262bp 5'-CAGAGGATGCTCTGTCATTG-3' and 5'-GGCTTGTTCTGAATGCACTG-3'); PECAM-1 (NM_000442.4; 172bp 5'-ATGATGCCCAGTTTGAGGTC-3' and 5'-ACGTCTTCAGTGGGGTTGTC-3'); FAK (NM_153831.3; 217bp 5'-CTGGCTACCCTGGTTCACAT-3' and 5'-TGTTGCTGTCGGATTAGACG-3'); Vimentin (NM_003380.3; 177bp 5'-GGGACCTCTACGAGGAGGAG-3' and 5'-AAGATTGCAGGGTGTTTTCG-3'); RACK1 (NM_006098.4, 226bp 5'-CTGAGTGTGGCCTTCTCCTC-3' and 5'-GCTTGCAGTTAGCCAGGTTC-3'); VE-Cadherin (NM_001795.3, 182bp 5'-CCAGGTATGAGATCGTGGTG-3' and 5'-

AAACAGAGAGCCCACAGAGG-3'); β2M (NM_004048.2, 158bp 5'-TTTCATCCATCCGACATTGAAG-3' and 5'-ACACGGCAGGCATACTCATC-3'); Clec14A (NM_175060.2, 198bp 5'-GACTTCCTCTGCCACTCCTC-3' and 5'-GGCTCAGGATCACTCTCCAG-3'); GAPDH (NM_002046.4, 228bp 5'-CGACCACTTTGTCAAGCTCA-3' and 5'-AGGGGTCTACATGGCAACTG-3'); α-tubulin (NM_006000.2, 207bp 5'-GACAGCTCTTCCACCCAGAG-3' and 5'-GGAGTGAGGTGAAGCCAGAG-3'); Rab11a (CR536493.1, 182bp 5'-CATGCTTGTGGGCAATAAGA-3' and 5'-TGTTTTCAGTGGTTGGTGGAAC-3'); Rab5c (CR541901.1, 250bp 5'-GAGTCTGCGGTAGGCAAATC-3' and 5'-CCCGTGCAAATGTATCTGTG-3'); and β-actin (NM_001101.3, 491bp 5'-CATCACCATTGGCAATGAGC-3' and 5'-CGATCCACACGGAGTACTTG-3'). RT-PCR was performed using an annealing temperature of 58^{o}C and an extension time of 30 seconds for 25 cycles. Amplicons were run on 2% agarose gels stained with GelRed (Phenix Research Products; Candler, NC).

EC Invasion Assay on 3D Collagen Gels

24 hours prior to use in a three dimensional invasion assay, ECs were fed with fresh growth medium, and M199 was equilibrated in a 10cm petri dish (5mL per T25 of ECs and 10mL per T75 of ECs) in an incubator at 37°C and 5% CO_2 overnight. On the day of the experiment, 1× HEPES buffered saline (20mM HEPES from Sigma-Aldrich; St. Louis, MO; and 150mM NaCl from J.T. Baker; Center Valley, PA; in sterile water), M199, and FBS were warmed in a water bath at 37°C for trypsinizing cells. Meanwhile,

three dimensional collagen I gels were prepared at 1mg/mL, 2.5mg/mL, and 5mg/mL as indicated with 1μM S1P (125μM stock solution suspended with 4mg/mL fatty acid-free BSA in sterile PBS; Sigma-Aldrich; St. Louis, MO) as reported previously (112). 20μg/mL of fibronectin (Sigma-Aldrich; St. Louis, MO) was added directly to the gels where indicated following the addition of S1P. The cold gel solution was added to wells of a half area 96-well plate (28μL each) and allowed to polymerize and equilibrate at 37°C and 5% CO_2 for 45 minutes. ECs were rinsed with 1× HEPES buffered saline and trypsinized as described (112). An aliquot of cells was counted and cell size was measured using a Cellometer® Auto 1000 cell counter (Nexcelom Bioscience LLC; Lawrence, MA). The cell pellet resulting from centrifugation following trypsinization was resuspended in equilibrated M199 containing RSII (1:250) as reported previously (84) at a density of 6×10^5cells/mL. 50μL of the cell suspension (30,000 cells) were added to each gel, and the cells were allowed to attach to the gels for 30 minutes at 37°C and 5% CO_2. Meanwhile cell feeding medium was prepared with 50μL of equilibrated M199 (per gel) containing RSII (1:250), 100μg/mL of sterile ascorbic acid (Sigma-Aldrich; St. Louis, MO), and 80ng/mL of VEGF and bFGF (R&D Systems; Minneapolis, MN). After 30 minutes, the cells were fed, the empty spaces surrounding the wells were filled with 165μL of sterile water to prevent evaporation, and the plate was placed in an incubator (37°C and 5% CO_2) for indicated amount of time. The cells were fixed in 200μL 3% glutaraldehyde (Sigma-Aldrich; St. Louis, MO) overnight or 200μL 4% paraformaldehyde (10mL 10% paraformaldehyde Electron Microscopy

Sciences; Hatfield, PA; and 2.5mL PBS in 12.5mL sterile water) for 20 minutes for immunofluorescent staining.

Immunoblotting

Total cell lysates of invading cultures were prepared by removing conditioned media and solubilizing gels containing invading ECs in boiling 1.5× Laemmli sample buffer at 100^{o}C for 10 minutes. Samples were separated using 8.5%-14% SDS-PAGE gels under reducing conditions (2% 2-mercaptoethanol, Sigma-Aldrich; St. Louis, MO) except when probing for β2M. The separated proteins were then transferred to Immobilon polyvinylidene fluoride membranes (Millipore; Billerica, MA), blocked with 5% nonfat dry milk at room temperature for 1 hour, and incubated with primary antibodies for 2 hours at room temperature (β_2M) or overnight at 4^{o}C. Antibodies against the following proteins were used for detection: β_2M (C7082, Sigma-Aldrich; St. Louis, MO) at 1:1500, annexin A2 (61008, BD Biosciences; San Jose, CA) at 1:1000, α-tubulin (T6199, Sigma-Aldrich; St. Louis, MO) at 1:10,000, GAPDH (ab8245, Abcam, Cambridge, UK) at 1:10,000, RACK1 (17754, Santa Cruz Biotechnology; Dallas, TX) at 1:3,000, VE-cadherin (sc52751, Santa Cruz Biotechnology; Dallas, TX) at 1:4,000, FAK (05-537, Millipore; Billerica, MA) at 1:4,000, PECAM-1 (3528s, Cell Signaling Technology; Danvers, MA) at 1,000, vimentin (sc-5565, Santa Cruz Biotechnology; Dallas, TX) at 1,2000, and actin (CP01, Calbiochem; Billerica, MA) at 1:1000. The membranes were then washed three times for 5 minutes in Tris-Tween 20 saline (150mM sodium chloride, 2.5mM Tris, 0.001% Tween® 20) before incubation with HRP

conjugated rabbit anti-mouse secondary antibody or goat anti-rabbit secondary antibody (1:5,000; Dako; Carpinteria, CA) in Tris-Tween 20 saline containing 5% milk for 1 hour. After three additional 5 minute washes, protein bands were visualized by adding Immobilon Western Chemiluminescent HRP Substrate (Millipore; Billerica, MA) for 5 minutes and exposing the membranes to HyBlot CL autoradiography film (Denville Scientific; South Plainfield, NJ). Films were developed with a FluorChem 8900 digital imaging system (Alpha Innotech; San Leandro, CA). For image quantification, band intensities were measured using NIH ImageJ image analysis software.

Immunofluorescence in 2D

Autoclaved glass coverslips (12mm round, #1.5; VWR; Radnor, PA) were placed in a 24-well plate and coated with 50µL of 20µg/mL collagen I prepared as in (112), fibronectin (Sigma-Aldrich; St. Louis, MO), Matrigel (Sigma-Aldrich; St. Louis, MO), or collagen IV (Sigma-Aldrich; St. Louis, MO) at 20µg/mL or 100µg/mL where indicated. After 20 minutes excess matrix solution was aspirated, and 50µL of ECs were seeded at 6×10^5cells/mL onto the coverslips (30,000 cells per coverslip). After a 30 minute incubation at 37^{o}C and 5% CO_2, the cells were fed with 1mL of growth medium overnight (37^{o}C and 5% CO_2). In the serum optimization study (Figure 2), the cells were wounded using a pipette tip attached to a vacuum and scratched in two directions creating an "X" pattern. The media was aspirated and the coverslips were rinsed twice with 500µL M199. Following wounding, the coverslips were serum-starved (placed in 250µL M199 for 2 hours) or placed in 250µL low serum media (2%) as indicated and

treated with 1μM S1P for indicated durations. Following treatment, the conditioned media was aspirated and replaced with 250μL 4% paraformaldehyde (10mL 10% paraformaldehyde Electron Microscopy Sciences; Hatfield, PA; and 2.5mL PBS in 12.5mL sterile water) for 20 minutes. The coverslips were washed twice with 500μL Tris-Glycine buffer (0.3% Tris and 1.5% Glycine) for 15 minutes each with gentle agitation, permeabilized with 500μL 0.5% Triton® X-100 in PBS for 20 minutes with gentle agitation, and blocked in 250μL goat-serum blocking buffer (0.1% Triton® X-100, 1% BSA, 1% goat serum, 0.2% Na Azide, and 1X TBS in sterile water) overnight at 4°C.

To stain the coverslips, primary antibodies were diluted in blocking buffer (25μL per coverslip), mixed by hand, and spun at 16,000×g for 1 minute. Antibodies used for 2D immunofluorescent staining include: VE-cadherin (sc-9989, Santa Cruz Biotechnology; Dallas, TX) at 1:200, VE-cadherin (ALX-210-232-C100, Enzo Life Sciences; Farmingdale, NY) at 1:200, ZO-1 (HPA001636, Sigma-Aldrich; St. Louis, MO) at 1:200, PECAM-1 (sc-1505, Santa Cruz Biotechnology; Dallas, TX) at 1:200, filamin A (1678, Millipore; Billerica, MA) at 1:300, paxillin (sc-365059, Santa Cruz Biotechnology; Dallas, TX) at 1:100, vinculin (V9131, Sigma-Aldrich; St. Louis, MO) at 1:100, phosphorylated focal adhesion kinase (FAK) at Y397 (ab4803, Abcam; Cambridge, UK) at 1:100, β-catenin (C7082, Sigma-Aldrich; St. Louis, MO) at 1:100, and α-catenin (C2081, Sigma-Aldrich; St. Louis, MO) diluted to 10mg/mL and used at 1:300. Meanwhile, a piece of Parafilm (American Can Company; Greenwich, CT) was stretched over the lid of a 24-well plate and labeled for treatment administered and

antibodies used. Following centrifugation, forming a dot without bubbles, 25µL per coverslip of the antibody dilutions were placed onto the Parafilm (one at a time). The coverslips were removed from the blocking buffer and the backside of the coverslip was dried before the coverslip was placed cell-side down onto the antibody dilution solution. The lid containing the coverslips was placed in a humidity chamber for 3 hours at room temperature. The coverslips were then washed with 500µL 0.1% Triton® X-100 in PBS for 10 minutes three times on an orbital shaker. In the dark, Alexa-488- or 594-conjugated secondary antibodies raised in goat (Molecular Probes; Grand Island, NY) were prepared (1:300) and placed on a new piece of Parafilm. From this point forward the coverslips were kept in the dark. Again the bottom surface of the coverslips were dried, placed cell-side down onto the antibody dilution dots, returned to a humidity chamber for 1 hour, and washed with 0.1% Triton® X-100 in PBS for 10 minutes three times. 50µL of 10µM 4',6-diamidino-2-phenylindole (DAPI) dye was added to the final wash for nuclear staining. During the washes, new FisherFinest Premium Frosted glass slides (Fisher Scientific; Waltham, MA) were cleaned with 70% ethanol using lint free tissue paper and labeled with a chemical resistant pen (VWR; Radnor, PA). When the coverslips were ready for mounting onto slides, one 15µL drop of Fluorogel with Tris Buffer mounting media (Electron Microscopy Sciences; Hatfield, PA) per coverslip was placed at a time onto each slide (up to four per slide). Following the last wash, the coverslips were rinsed three times in distilled deionized water. The backside of the each coverslip was dried before it was placed cell-side down onto a Fluoro-gel dot. The slides were kept in the dark at room temperature overnight. The next morning the coverslips

were sealed for long term preservation by tracing the outline of each coverslip with clear nail polish. After drying, the coverslips were imaged using a Nikon TI A1R inverted confocal microscope and stored in dark at 4^{o}C until further use. All images were taken as Z-stacks with a step size of 0.4µm at 60× magnification and are displayed as extended depth of focus (EDF) images.

Immunofluorescence in 3D

Conditioned media was removed from collagen gels in a half area 96-well plate containing invading cells and replaced with 200µL 4% paraformaldehyde for 20 minutes. Following fixation, the gels were washed twice with 200µL Tris-Glycine buffer for 15 minutes each with gentle agitation, removed from the 96-well plate, sliced using a razor blade and placed in a 24-well plate with 1mL 0.5% Triton® X-100 in PBS to permeabilize for 20 minutes with gentle agitation. The gels were then blocked in 1mL goat-serum blocking buffer overnight at 4^{o}C.

To stain the gels, primary antibodies were diluted in goat-serum blocking buffer (100µL per gel), mixed by hand, and spun at 16,000g for 1 minute. Antibodies used for 3D immunofluorescent staining include: VE-cadherin (sc-9989, Santa Cruz Biotechnology; Dallas, TX) at 1:200 and ZO-1 (HPA001636, Sigma-Aldrich; St. Louis, MO) at 1:200. Either whole gels or gel slices were then placed in a 96-well plate with the primary antibody dilution on a shaker for 3 hours. For washing, the gels were transferred to a 24-well plate containing 1mL 0.1% Triton® X-100 in PBS and placed on a shaker for two 30 minute washes. In the dark, goat Alexa-488- or 594-conjugated

secondary antibodies (Molecular Probes; Grand Island, NY) were prepared in goat-serum blocking buffer (1:300), placed in a 96-well plate with the gels, and set on a shaker for 1 hour. Again, for washing, the gels were transferred to a 24-well plate containing 1mL 0.1% Triton® X-100 in PBS and placed on a shaker for two 30 minute washes and an overnight wash. The next day the wash buffer was changed again and 100µL of 10µM DAPI was added for 30 minutes on the shaker. Meanwhile, FisherFinest Premium Frosted glass slides (Fisher Scientific; Waltham, MA) and coverglasses (24×50mm, #1.5; VWR; Radnor, PA) were cleaned with 70% ethanol using lint free tissue paper and labeled with a chemical resistant pen (VWR; Radnor, PA). Additionally, silicone 0.04" thick (Specialty Manufacturing Incorporated; Pineville, NC) was cut to the same size as the coverglass, and a hole punch was used to create wells for the gels. Fluorogel with Tris Buffer mounting media (Fluorogel; Electron Microscopy Sciences; Hatfield, PA) was then used to adhere the silicone to the slide and allowed to dry briefly (about 30-60 minutes). The wells were then filled with Fluorogel and the gels were oriented so that the monolayer or invading structures could be imaged by confocal microscopy. Finally, to minimize bubbles formed in the wells with the gels, a layer of Fluorogel was spread across the top of the silicone and the coverglass was gently placed on top. The slides were allowed to dry overnight in the dark before imaging with a Nikon TI A1R inverted confocal microscope. All images were taken as Z-stacks with a step size of 0.4µm or 1µm as indicated at 40× magnification and are displayed as EDF focused images.

Junctional Width Quantification

Utilizing NIS-Elements AR 4.0 (Nikon), confocal EDF focused images of two dimensional EC monolayers stained with VE-cadherin were analyzed to determine average junctional width. At least six images per treatment group (shβ2M-1, shANXA2-2) each containing 20 cells were analyzed for three independent experiments. A blinded volunteer chose a representative cell for each image and collected five measurements equally across each junction of the representative cell for a total of at least 150 measurements per treatment group per experiment. The lengths of these lines in microns were exported to Microsoft Excel for analysis.

Focal Adhesion Quantification

Confocal EDF focused images of two dimensional EC monolayers stained with paxillin and converted to .tif files were read by a MATLAB program written generously by Dr. Po Feng Lee for the quantification of focal adhesions. The program amplified the signal in the images, set a threshold, and created a mask to eliminate all background information that did not meet the threshold. Output data consisted of total focal adhesion number and size in pixels per image. At least two images containing 20 cells each per treatment group were analyzed for three independent experiments.

Reticular Junction and Mean Fluorescence Intensity Quantification

Confocal EDF focused images of two dimensional EC monolayers stained with VE-cadherin and ZO-1 were analyzed to determine average number of reticular

junctions and relative amounts of VE-cadherin and ZO-1 protein expression over time. All junctions containing a "honeycomb" pattern of VE-cadherin staining were counted manually for at least two images per cell type (shβ_2M-1 and shANXA2-1) or timepoint (0.25 hours, 4 hours, 8 hours, 12 hours) for two-three independent experiments. Average fluorescence intensity was quantified using the Histogram function in NIS-Elements AR 4.0 (Nikon). The mean intensity of either the red (VE-Cadherin) signal or the green (ZO-1) signal was quantified from snapshots of confocal EDF focused images for at least two images per timepoint for two independent experiments.

Mouse Tissue Analysis

Uterine decidual tissue was harvested from Sv/129 Pas mice at day 7.5 of pregnancy and imbedded in optimal cutting temperature compound (OCT, Sakura; Torrance, CA) and frozen at -80^{o}C until needed. Sections 30μm thick were incubated for 10 minutes in methanol at -20^{o}C. The OCT was removed from the sections using forceps, and each section was outlined with a hydrophobic slide marker (Research Products International Corporation; Mt Prospect, IL). The slides were rinsed briefly in 0.3% Tween in PBS, dried, and blocked in goat-serum blocking buffer for 1 hour at room temperature. Meanwhile, primary antibodies were diluted in goat-serum blocking buffer, mixed by hand, and spun at 16,000g for 1 minute. Again the slides were rinsed briefly in 0.3% Tween in PBS, and 30μL of primary antibody dilutions were added to each section. Antibodies used for mouse tissue immunofluorescent staining include: PECAM-1 (553371, BD Pharmingen; San Jose, CA) at 1:200 and α-catenin (C2081,

Sigma-Aldrich; St. Louis, MO) diluted to 10mg/mL and used at 1:200. The slides were then placed in a humidity chamber and incubated overnight at 4°C. The slides were washed three times in 0.3% Tween in PBS for 10 minutes each and in the dark, goat Alexa-488- or 594-conjugated secondary antibodies (Molecular Probes; Grand Island, NY) were prepared in goat-serum blocking buffer (1:250), 30µL per section. The slides were incubated for 1 hour at room temperature in a humidity chamber. Finally, the sections were washed four times for 10 minutes each in 0.3% Tween in PBS. The sections were rinsed briefly with water and a glass coverslip was added with DAPI-countaining mounting media (P36935; Invitrogen; Carlsbad, CA). The next morning the coverslips were sealed for long term preservation by tracing the outline of each coverslip with clear nail polish. After drying, the coverslips were imaged using a Nikon TI A1R inverted confocal microscope and stored in dark at 4°C until further use.

Statistical Analysis

Data are presented as the mean ± S.D. for each group of samples. Statistical analyses were performed using Microsoft Excel. Comparisons were performed using Student's *t*-tests. $P<0.05$ was considered statistically significant.

CHAPTER III

RESULTS

Previously our lab demonstrated a decrease in the invasive capacity and an increase in the permeability of cells lacking the ANXA2 protein (108). Throughout this study, we explore the effect ANXA2 silencing has on EC junctions. First, we characterized changes in RNA and protein expression in ECs transduced with lentiviruses delivering short hairpin RNA (shRNA) directed to control (β2M) or ANXA2. We tested two shRNA clones for each protein. Figure 1A illustrates the relative mRNA levels of over a dozen proteins supporting there are no off target effects of the short hairpin RNAs on many junctional and cytoskeletal proteins we and others have shown to been important in EC sprouting. While β2M and ANXA2 were silenced, levels of GAPDH, α-tubulin, actin, RACK1, VE-cadherin, Vimentin, PECAM-1, FAK, RAB11a, RAB5c, and Clec14A were not affected. Appropriate silencing was also observed for β2M and ANXA2 at the protein level, while expression of many junctional and cytoskeletal proteins GAPDH, α-tubulin, actin, RACK1, VE-cadherin, Vimentin, PECAM-1, and FAK remained constant (Figure 1B). These data support that shRNA-mediated silencing of β2M and ANXA2 is specific. Clone 1 for both the control or β2M group (shβ2M-1) and the ANXA2 group (shANXA2-1) exhibited the most complete silencing of the desired proteins and were used for subsequent experiments where indicated.

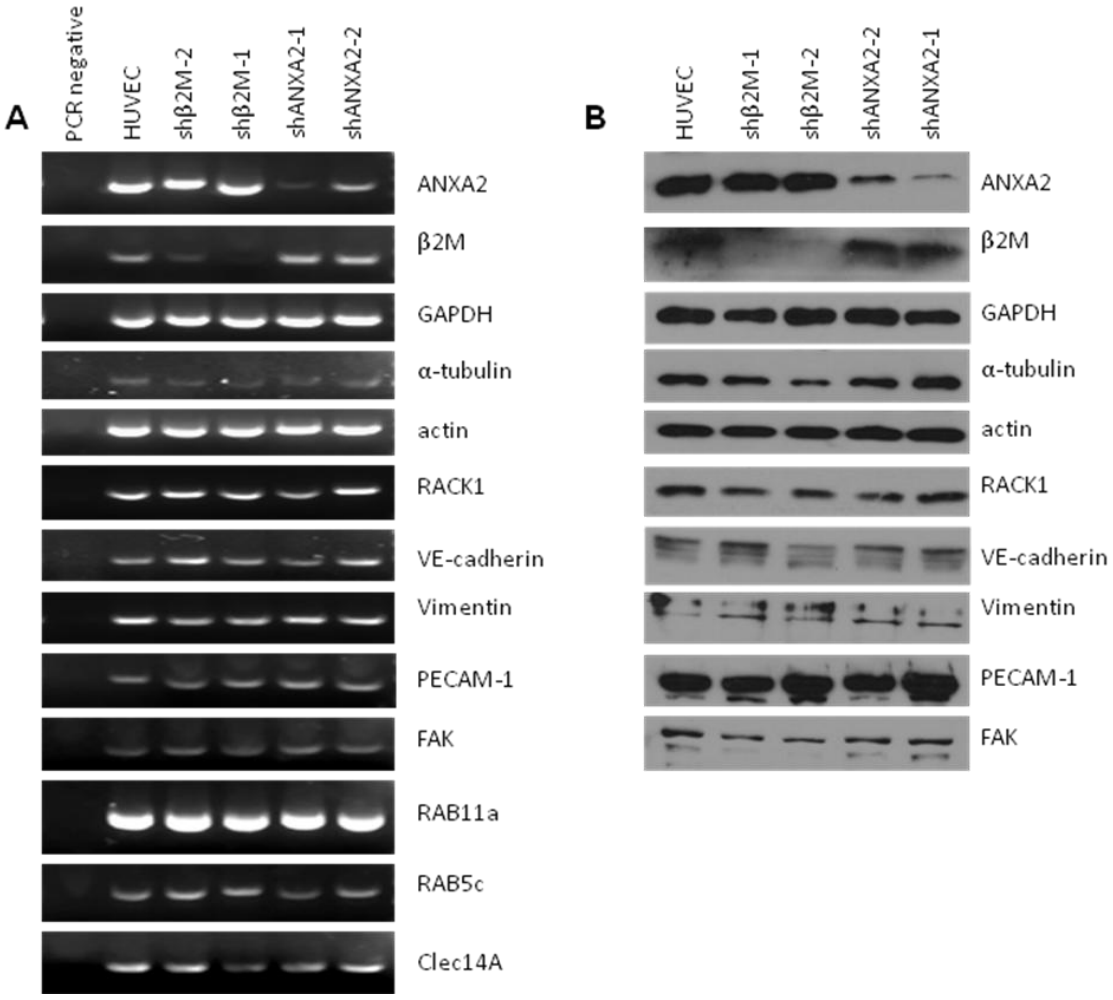

Figure 1. Transduction of endothelial cells with shRNA specifically reduced mRNA and protein levels for shβ2M and shANXA2.
(A) Non-transduced ECs (HUVEC), or ECs transduced with lentiviruses delivering shRNA directed to β2-microglobulin (shβ2M-1 and -2) or annexin A2 (shANXA2-1, and -2) were utilized to make RNA for cDNA synthesis and amplified via RT-PCR using ANXA2-, β2M-, GAPDH-, α-tubulin-, actin-, RACK1-, VE-cadherin-, Vimentin-, PECAM-1-, FAK-, RAB11a-, RAB5c-, and Clec14A-specific primers. **(B)** Cell lysates from treatment groups as in A were analyzed by western blotting using ANXA2-, β2M-, GAPDH-, α-tubulin-, actin-, RACK1-, VE-cadherin-, Vimentin-, PECAM-1-, and FAK-specific antisera.

Next, we observed the morphology of the knockdown cells at confluence. As shown in Figure 2A, similar to non-trasnduced ECs (HUVEC), the ECs lacking control, β2M, or ANXA2 proteins exhibit a "cobblestone" morphology. Additionally, following trypsinization of the ECs, the average cell diameter in microns was quantified by a Nexcelom Cellometer Auto 1000 cell counter. Data in Figure 2B show the average cell diameter is not different between HUVEC, shβ2M-1, or shANXA2-1 expressing cells.

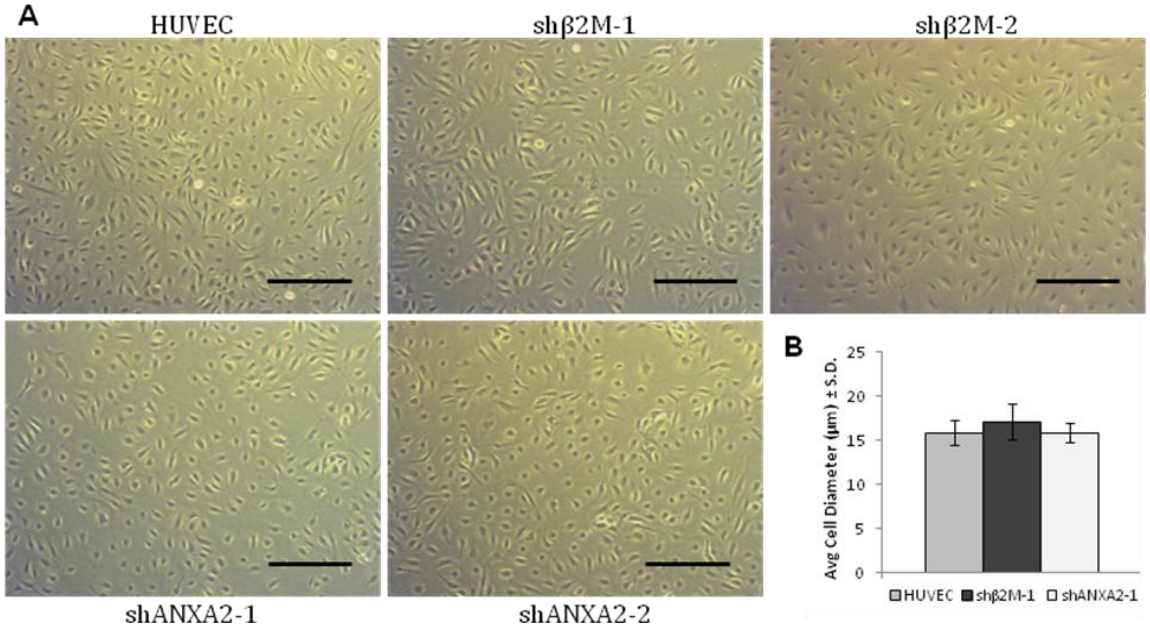

Figure 2. Lentiviral transduction with shRNA directed to β2M and ANXA2 does not significantly alter EC morphology.
(A) Representative phase images illustrating the cobblestone morphology of confluent endothelial cells. Cells were seeded in gelatin coated tissue cultured flasks and imaged 4 days after transduction. From left to right; Non-transduced ECs (HUVEC), shβ2M-1, shβ2M-2 (upper panels), and shANXA2-1, shANXA2-2 (lower panels). Scale bar = 100μm. **(B)** Average cell diameter following cell trypsinization in microns was quantified for three independent experiments using Nexcelom Cellometer Auto 1000 software. Data represent average of averages ± S.D. of over 150 total cells/group. There was no significant difference in size between groups.

Because VE-cadherin is critical for ensuring endothelial integrity, we hypothesized ANXA2 silencing may affect localization of VE-cadherin. To visualize protein localization, ECs were seeded onto collagen-I coated glass coverslips and analyzed by immunofluorescent staining. The cells were seeded at confluence and were allowed to attach overnight. In subconfluent monolayers ECs were elongated, highly motile, proliferative, and sensitive to growth factor stimulation (113). ECs were seeded at confluence to achieve a resting or quiescent morphology where contact with neighboring cells inhibits cell activation (114). At confluence the junctions are stabilized, and junctional proteins are able to transduce signals, such as that from S1P, across the monolayer contributing to gene expression changes (115-117). After 18 hours, the cells were serum starved for two hours to ensure cell quiescence and treated for one hour with 1μM S1P, known to fortify junctional proteins including VE-cadherin (36). Following treatment, the cells were fixed, rinsed, permeabilized, blocked, stained with primary antibodies directed to desired proteins and secondary antibodies conjugated to Alexa 488 or 594, and analyzed with confocal microscopy. Figure 3 illustrates relative VE-cadherin localization in non-transduced ECs (HUVEC) and ECs expressing shRNA directed to β2M (shβ2M-1 and -2) and ANXA2 (shANXA2-1 and -2). The HUVEC and shβ2M groups showed a thin, linear distribution of VE-cadherin at the cell-cell junctions, while the ANXA2 knockdown cells exhibited a wider and less linear distribution. Additionally, the shANXA2-1 cells exhibited a more consistent wide VE-cadherin localization than the shANXA2-2 cells suggesting that there is a correlation between the amount of ANXA2 present in the cells and the localization of VE-cadherin.

For the following experiments, we examine the localization of other junctional proteins in ECs expressing shβ2M-1 and shANXA2-1 to determine if the localization of other proteins is altered.

Figure 4 displays representative photos for shβ2M-1 and shANXA2-1 cells stained for several protein members of adherens junctions, specifically, VE-cadherin, PECAM-1, and filamin A. The trend of a wider junctional protein distribution in the shANXA2-1 group appears consistent for each of the junctional proteins, VE-cadherin, PECAM-1, and filamin A, suggesting ANXA2 is required for the formation and/or maintenance of linear adherens junctions in response to S1P.

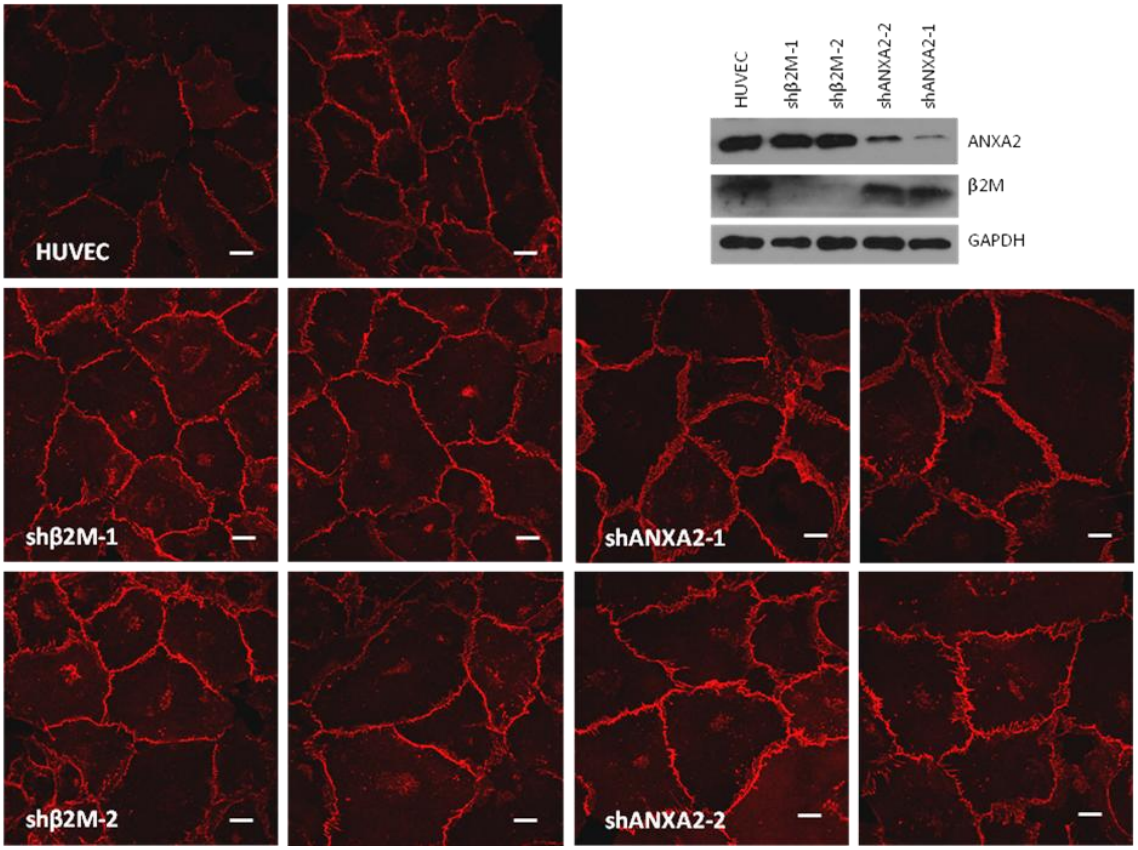

Figure 3. VE-cadherin distribution changes with ANXA2 silencing.
Representative confocal extended depth of focus (EDF) images (2 images per group are shown) illustrating the localization of VE-cadherin. Left two panels from top to bottom, Non-transduced ECs (HUVEC), shβ2M-1, and shβ2M-2, Right two panels from top to bottom; shANXA2-1 and shANXA2-2. ECs expressing shβ2M or shANXA2 were seeded on collagen I-coated glass coverslips overnight. After 18 hours cells were serum starved for 2 hours, treated with 1μM S1P for 1 hour, fixed, and stained for VE-cadherin-specific antisera and corresponding secondary antibodies conjugated to Alexa 594. Western blots showing appropriate knockdown of β2M or ANXA2 are from a separate independent experiment. Scale bar = 10μm.

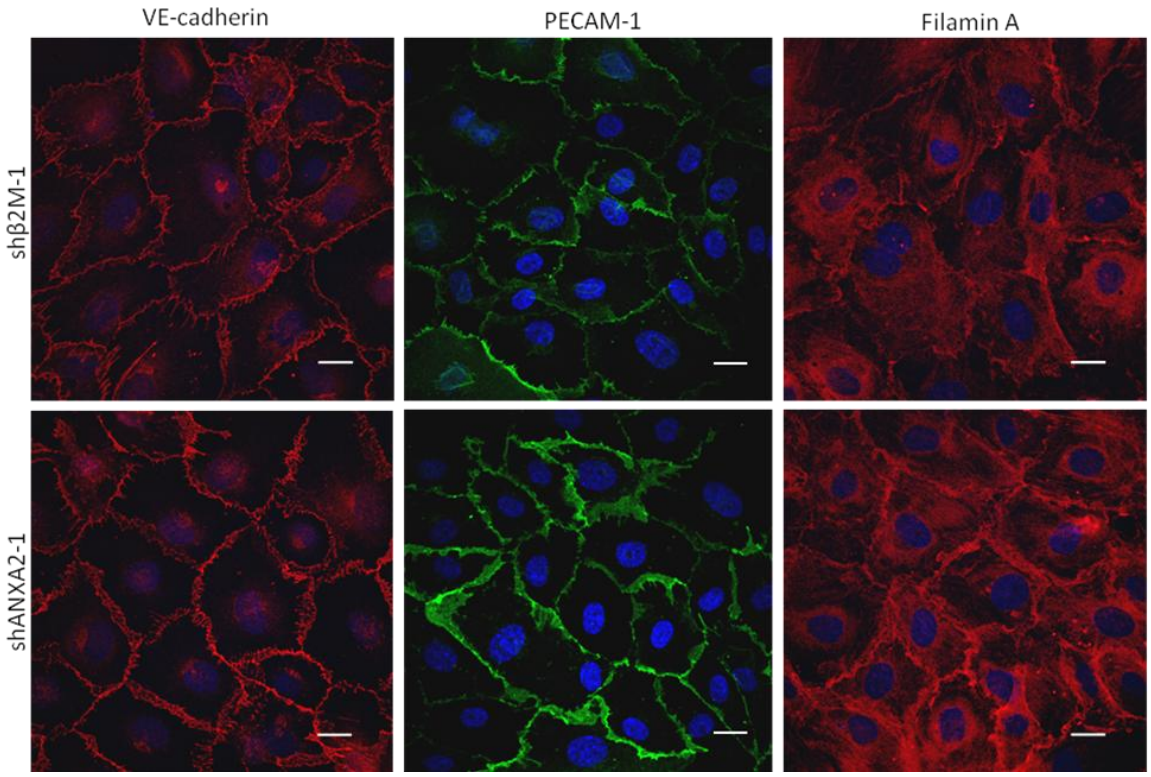

Figure 4. Knockdown of ANXA2 alters junctional protein localization.
Representative confocal EDF images illustrating from left to right the localization of VE-cadherin, PECAM-1, and filamin A with ANXA2 knockdown. shβ2M-1, upper panels; shANXA2-1, lower panels. ECs expressing shβ2M or shANXA2 were seeded on collagen I-coated glass coverslips overnight. After 18 hours cells were serum starved for 2 hours, treated with 1μM S1P for 1 hour, fixed, and stained with primary antibodies directed to VE-cadherin, PECAM, or filamin A. Secondar antibodies used were conjugated to Alexa 594 (VE-cadherin and filamin A) or Alexa 488 (PECAM-1). Nuclei were stained with 1μM DAPI (blue). Scale bar = 10μm.

Following the observation of wider cell-cell junctions, we characterized the change by quantifying the junctional width using the NIS Elements software by Nikon. At least three confocal EDF images were taken for each group, shβ2M-1 and shANXA2-1, for each of three independent experiments. After the number of cells per image was quantified to ensure equal confluency across the groups (Figure 5B), a blinded volunteer viewed the series of randomized confocal images. After choosing a representative cell for each image, five measurements of junctional width equidistant along each junction of the representative cell were recorded (Figure 5A). The average junctional width was quantified in microns for over 60 total junctions per group and plotted as mean junctional width (Figure 5C) and median junctional width (Figure 5D). The data revealed that the average junctional width for shANXA2-1 cell-cell junctions was almost twice that of the shβ2M-1 cell-cell junctions.

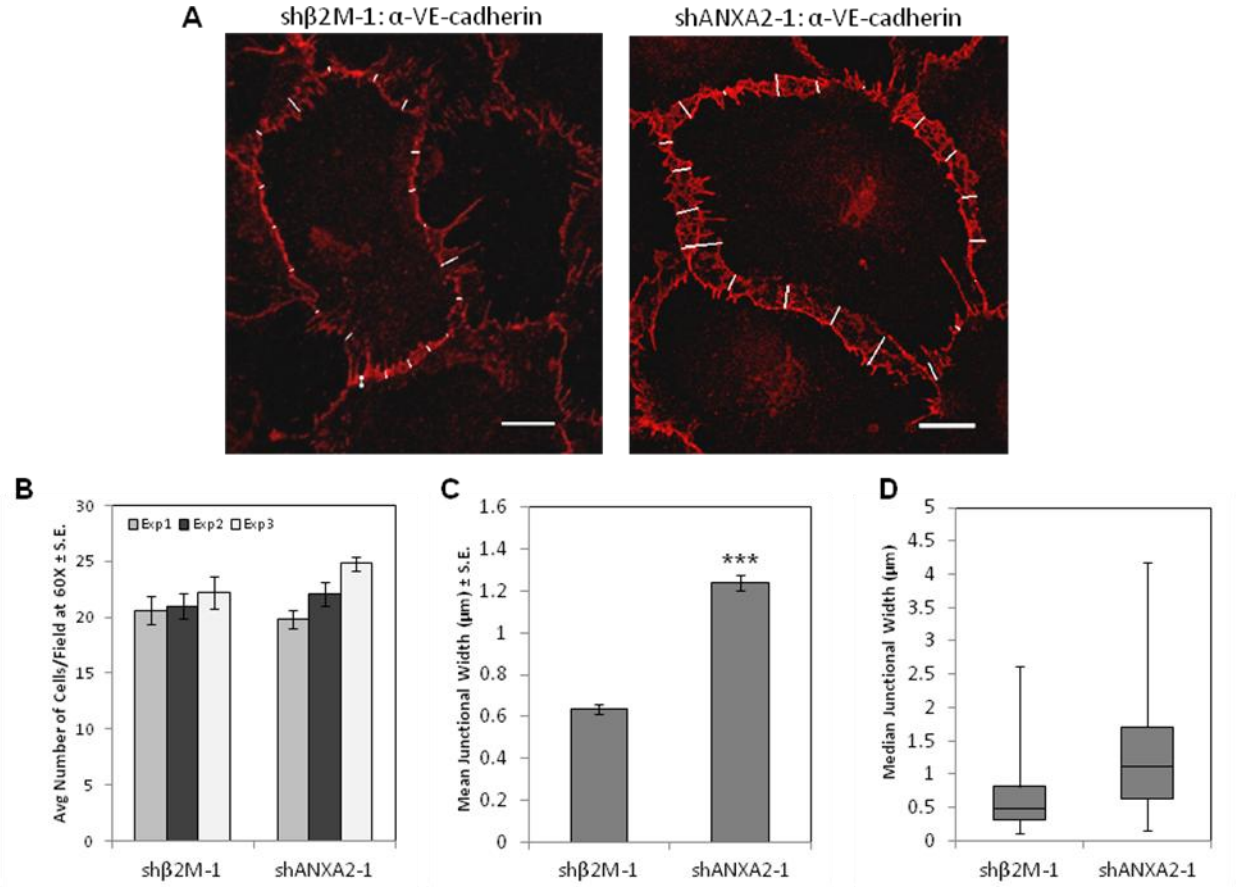

Figure 5. Knockdown of ANXA2 increases EC junction width.

(A) Confocal EDF images illustrating how the junction width was quantified using digital images of ECs stained for VE-cadherin as shown in Figure 3. ECs expressing shβ2M or shANXA2 were seeded on collagen I-coated glass coverslips overnight. After 18 hours cells were serum starved for 2 hours, treated with 1μM S1P for 1 hour, fixed, and stained for VE-cadherin. In a blind study, five measurements of junctional width were taken equidistant apart along each edge of a representative cell. Scale bar = 5μm. **(B)** To ensure equal cell density, the average number of cells per field was quantified from images captured using a 60X objective. Data represent average number of cells per field ± S.E. of at least 7 fields per group for three independent experiments. There was no significant difference between the shβ2M-1 and shANXA2-1 groups. (C, D) Data represent average junction width in microns ± S.E. and median junctional width displaying the minimum and maximum junctional width quantified for three independent experiments using NIS Elements software. Data represent analyses of more than 60 total junctions/group. (Student's *t*-test, ∗∗∗ $p<0.0001$).

The adherens junction is fortified by catenins, specifically, α-, β-, and p120-catenin, which bind to adherens junction proteins and protect them from endocytosis (73). S1P enhances the interaction between VE-cadherin and both α- and β-catenin (57), further solidifying the adherens junction complex at the EC membrane. To determine if ANXA2 is required for the interaction of catenins with the adherens junction, we tested for VE-cadherin and α-catenin colocalization in ECs expressing shβ2M-1 and shANXA2-1 (Figure 6). VE-cadherin and α-catenin colocalized similarly in both groups of cells, suggesting that ANXA2 is not required for S1P-induced association of α-catenin and VE-cadherin, and the effect of ANXA2 knockdown on junctional widening is independent of catenin association with VE-cadherin.

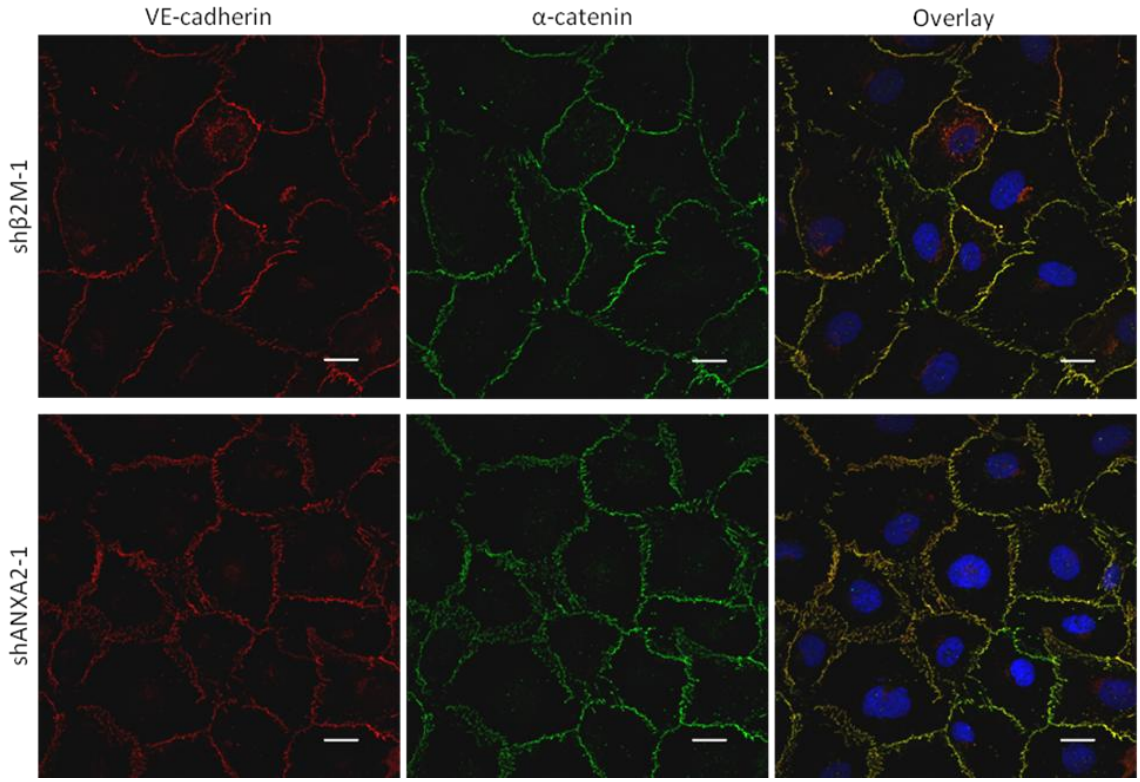

Figure 6. Knockdown of ANXA2 does not affect α-catenin association with VE-cadherin.

Representative confocal EDF images illustrating from left to right the localization of VE-cadherin and α-catenin. The far right panel is an overlay of the images. shβ2M-1, upper panels; shANXA2-1, lower panels. HUVECs expressing shβ2M or shANXA2 were seeded on collagen I-coated glass coverslips overnight. After 18 hours cells were serum starved for 2 hours, treated with 1μM S1P for 1 hour, fixed, and stained with primary antibodies directed to VE-cadherin and α-catenin and corresponding secondary antibodies conjugated to Alexa 594 and Alexa 488, respectively. Nuclei were stained with 1μM DAPI (blue). Scale bar = 10μm.

After discovering the effects ANXA2 silencing had on the distribution of junctional proteins, we hypothesized similar effects may be seen with focal adhesion proteins, because Garcia and colleagues reported that S1P stimulated the association of focal adhesion proteins, including focal adhesion kinase (FAK) and paxillin, with EC junctions (57). To confirm this, we characterized focal adhesion protein responses to S1P by seeding confluent EC monolayers overnight onto collagen I coated glass coverslips. Following brief (2 hour) serum starvation, ECs were treated with 1μM S1P for 1 hour. In addition to FAK and paxillin, we tested the effect of S1P on vinculin localization. Vinculin is another focal adhesion protein that has also been shown to associate with cell-cell junctions (118). Figure 7 displays an increase in focal adhesion protein localization to cell-cell junctions following the addition of S1P. While phosphorylated FAK(Y397) and paxillin staining are consistent with the literature (57), an increase in vinculin localization to the cell-cell junctions with S1P has not been shown previously. Interestingly, vinculin appears to localize to punctate focal adhesion structures as well as linear junctional structures.

Once we defined the effects of S1P on focal adhesion protein localization to EC junctions, we tested whether silencing of ANXA2 would alter the localization focal adhesion proteins to EC junctions in response to S1P. ECs expressing shβ2M-1 and shANXA2-1 were seeded at confluence, serum starved, treated with S1P, and analyzed by immunofluorescent staining as in Figure 3. As shown in Figure 8, vinculin, pFAK(Y397), and paxillin were localized in large focal adhesion structures near the cell-cell junctions in the control (shβ2M-1). Vinculin localization did not change overtly in

the absence of ANXA2, although the presence of a wide junctional localization of vinculin in the shANXA2-1 cells is noteworthy, confirming the dual role of vinculin as both a focal adhesion and junctional protein that interacted with VE-cadherin (118). In contrast to vinculin, paxillin- and pFAK-positive focal adhesions appeared smaller in the shANXA2-1 cells.

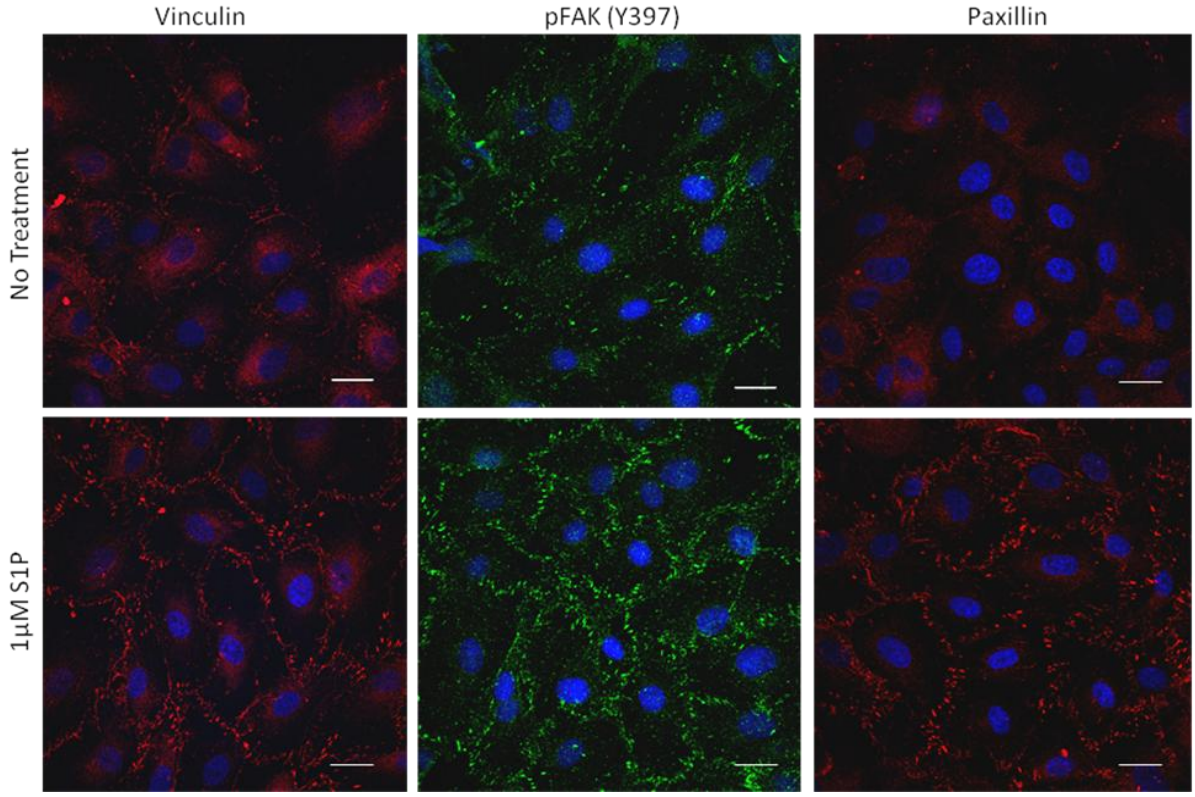

Figure 7. S1P stimulates focal adhesion protein localization to junctions.
Representative confocal EDF images from one of three independent experiments illustrating that S1P causes vinculin, phosphorylated FAK (Y397), and paxillin to move to cell-cell junctions. HUVECs were seeded onto collagen I-coated glass coverslips overnight. After 18 hours cells were serum starved for 2 hours, and either left untreated (upper panels) or treated with 1μM S1P (lower panels) for 1 hour, fixed, and stained with primary (and corresponding secondary) antibodies directed to, from left to right, vinculin (119), pFAK (Alexa 488), and paxillin (119). Nuclei were stained with 1μM DAPI (blue). Scale bar = 10μm.

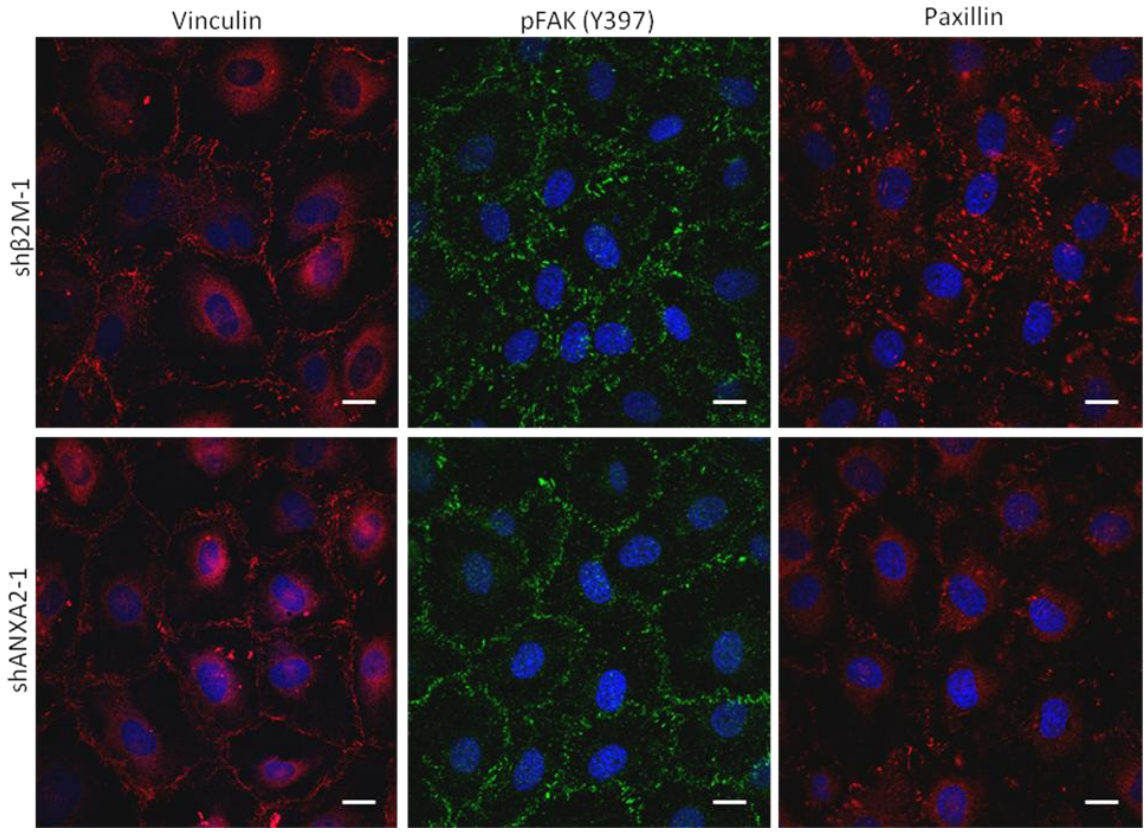

Figure 8. Knockdown of ANXA2 alters S1P-induced focal adhesion protein localization to cell-cell junctions.
Representative confocal EDF images illustrating from left to right the localization of vinculin, FAK phosphorylated at Y397, and paxillin with ANXA2 knockdown. shβ2M-1, upper panels; shANXA2-1, lower panels. ECs expressing shβ2M or shANXA2 were seeded on collagen I-coated glass coverslips overnight. After 18 hours cells were serum starved for 2 hours, treated with 1μM S1P for 1 hour, fixed, and stained as shown in Figure 7. Scale bar = 10μm.

To confirm the punctate structures near the junctions were focal adhesions, we costained ECs expressing shβ2M-1 and shANXA2-1 with paxillin and pFAK. Figure 9 shows a magnified image of the focal adhesions near the junctions. Both proteins localized to large focal adhesions in the shβ2M-1 cells. In the shANXA2-1 cells, however, the focal adhesions were much smaller and appear to have much less paxillin and pFAK.

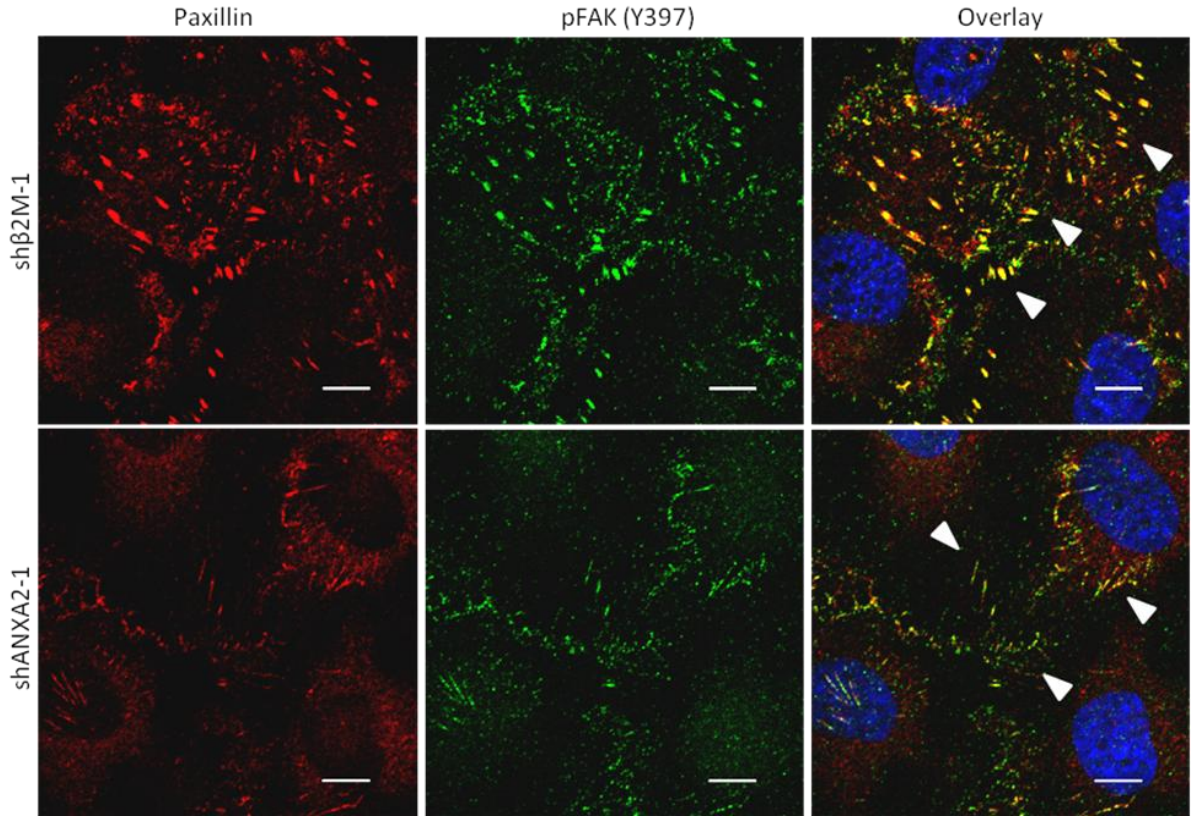

Figure 9. ANXA2 knockdown reduces focal adhesion size near endothelial junctions.

Representative confocal EDF images from one of three independent experiments illustrating that focal adhesions indicated by pFAK (Y397) and paxillin, appear smaller near EC junctions when ANXA2 expression is knocked down. ECs expressing shβ2M-1 or shANXA2-1 were seeded on collagen I-coated glass coverslips overnight. After 18 hours cells were serum starved for 2 hours, treated with 1μM S1P for 1 hour, fixed, and stained with primary antibodies directed to pFAK and paxillin and corresponding secondary antibodies conjugated to Alexa 488 and 594, respectively. Nuclei are stained with 1μM DAPI (blue). Arrowhead indicates focal adhesions near endothelial junctions. Scale bar = 5μm.

To confirm this we quantified focal adhesion size using MATLAB. Confocal EDF images were input into a MATLAB program generously written by Dr. Po Feng Lee for the quantification of focal adhesion size. Figure 10A displays the steps the program takes to prepare the images for quantification. The image is read by the program; the detected signal is amplified; a mask is applied to eliminate the background signal; and the focal adhesion sizes are measured and quantified. Focal adhesion sizes were measured for both shβ2M-1 and shANXA2-1 cells stained for paxillin. A twelve percent reduction in size was detected from focal adhesions in the control group compared to the shANXA2-1 group (Figure 10B). This indicates that ANXA2 is required for the S1P-induced localization of focal adhesion proteins, specifically paxillin, to large focal adhesions near cell-cell junctions.

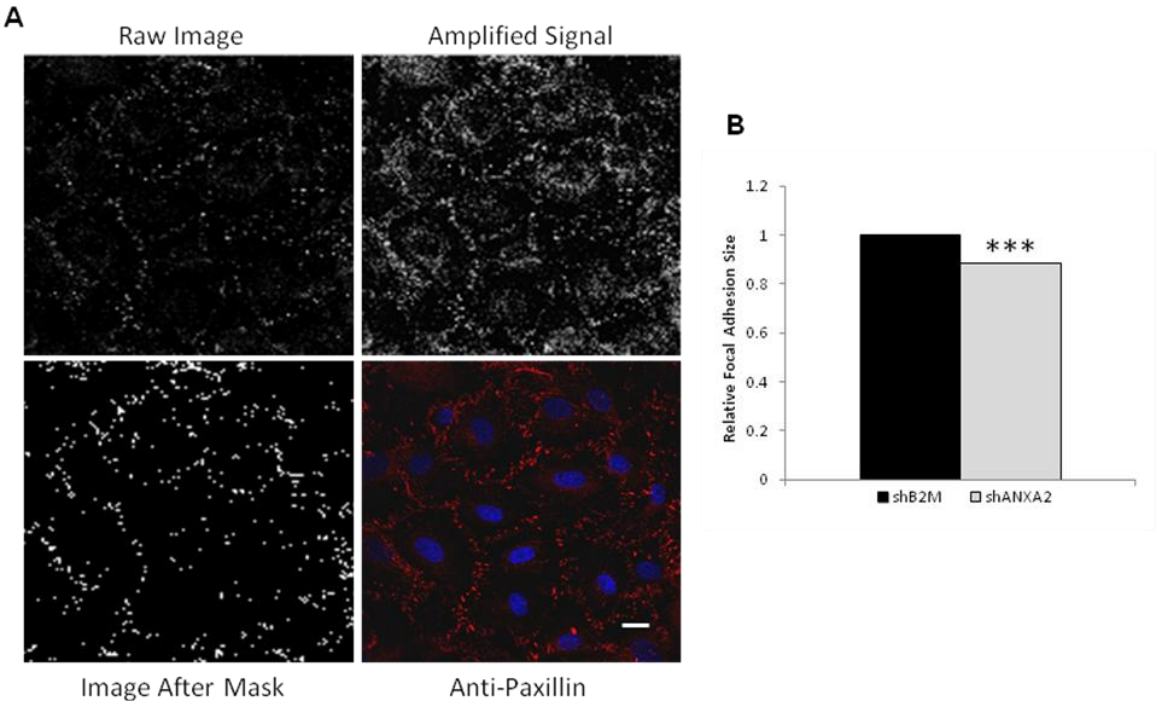

Figure 10. Knockdown of ANXA2 reduces focal adhesion size.
(A) Representative images and original confocal EDF image illustrating how the focal adhesion size was quantified using MATLAB software. ECs expressing shβ2M or shANXA2 were seeded on glass coverslips overnight. After 18 hours cells were serum starved for 2 hours, treated with 1μM S1P for 1 hour, fixed, and stained for paxillin. Confocal EDF images were analyzed by MATLAB. Scale bar = 10μm. From left to right, the raw image, the image after amplification (upper panels), the amplified image after application of a mask eliminating background, and the original image for comparison (lower panels). **(B)** Relative average focal adhesion size for three independent experiments. Data represent analyses of more than 11,000 total focal adhesions/group. (Student's *t*-test, ＊＊＊ $p<0.0001$).

After testing the effects ANXA2 silencing on the localization of various junctional and focal adhesion proteins, we performed additional co-stains to further examine which proteins might colocalize at the junction. These studies, shown in Figure 11, revealed that the wide portions of the shANXA2-1 cell-cell junctions showed a "honeycomb" pattern when stained for VE-cadherin, β-catenin, or PECAM-1. This pattern of VE-cadherin and PECAM-1 staining in ECs has been reported as a "reticular junction" in unstimulated HUVECs cultured on fibronectin coated coverslips for more than 48 hours (109). While PECAM-1, VE-cadherin and β-catenin localized to reticular areas, ZO-1 and paxillin did not. Reticular junctions are indicated by arrowheads. Following identification of the shANXA2-1 EC junctions as "reticular," we had a blinded volunteer quantify the number of reticular junctions in shβ2M-1 and shANXA2-1 groups as indicated by the "honeycomb" pattern of VE-cadherin staining. At least 7 images were quantified for each cell type in each of three independent experiments. Figure 12 displays representative photos from the two groups and the quantification of the reticular junctions illustrating the shANXA2-1 cells had almost six times the number of reticular junctions as the shβ2M-1 cells.

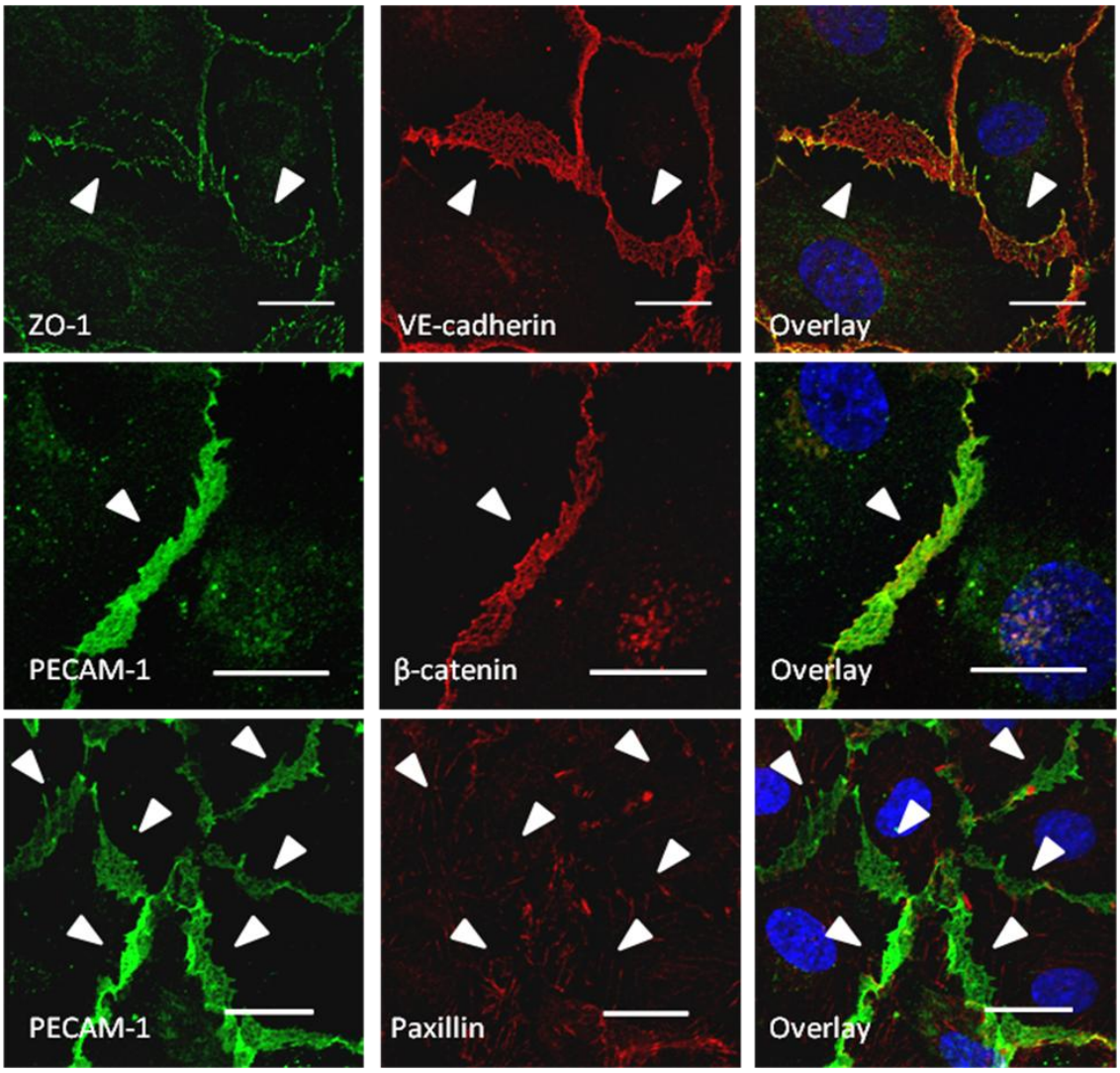

Figure 11. Close up of co-stains of shANXA2-1 cells to illustrate reticular junctions. Representative confocal EDF images showing co-stains of the indicated proteins in shANXA2-1 cells following a two hour serum starve and 1 hour 1μM S1P treatment as detailed in Figure 3. VE-cadherin, PECAM-1, and β-catenin stains exhibit a "honeycomb" or reticular pattern at the EC junctions. ZO-1, a tight junction protein, did not colocalize with VE-cadherin (top panels). The middle panels show colocalization of PECAM-1 and β-catenin at the EC junctions; however, as expected, paxillin did not colocalize with PECAM-1 (lower panels). Arrowheads indicate reticular junctions. Scale bar = 10μm.

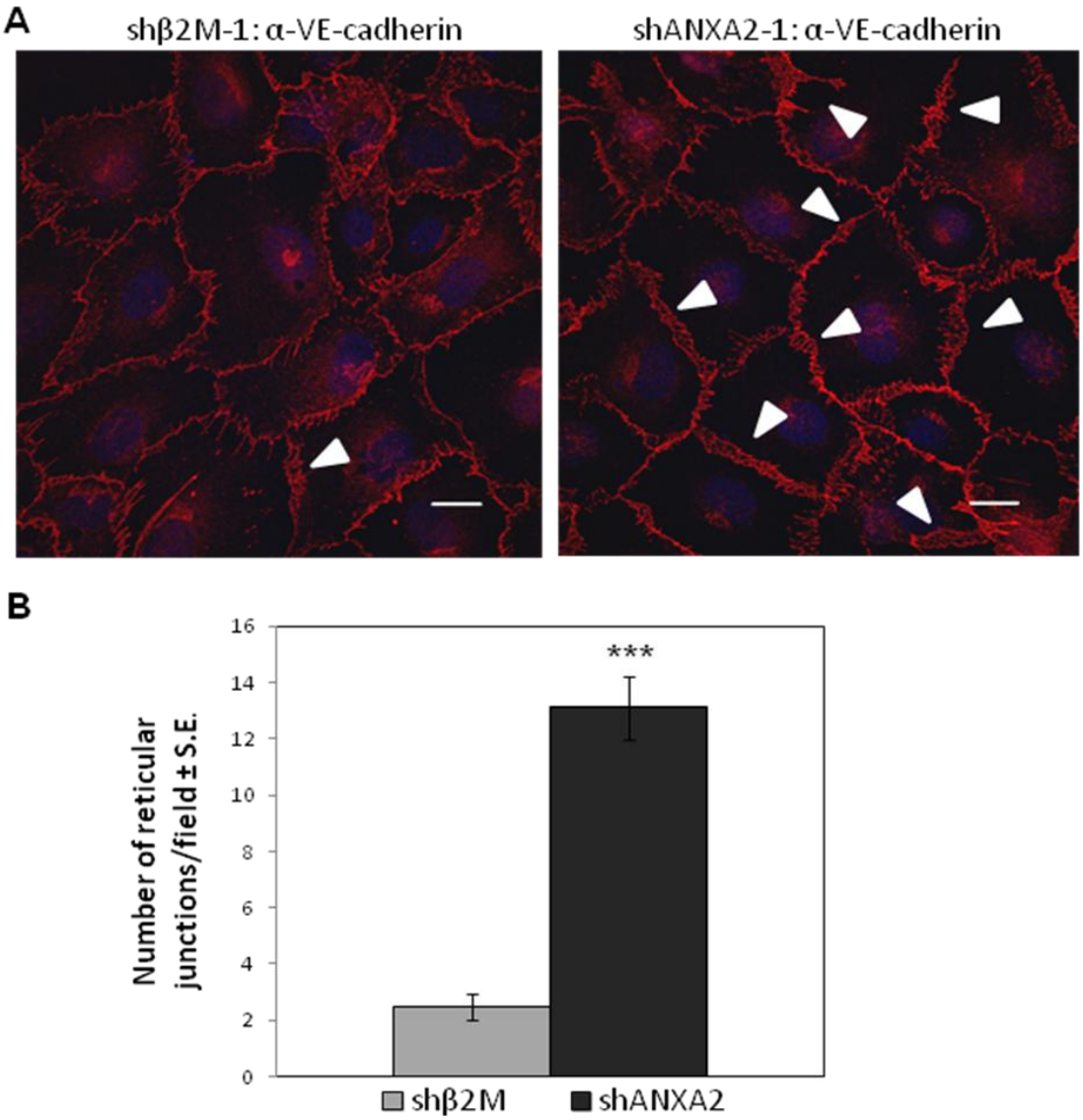

Figure 12. shANXA2-1 cells have more reticular junctions than shβ2M-1 cells. **(A)** Confocal EDF images illustrating how the reticular junctions were quantified using digital images of ECs stained for VE-cadherin as shown in Figure 3. ECs expressing shβ2M-1 or shANXA2-1 were seeded on collagen I-coated glass coverslips overnight. After 18 hours cells were serum starved for 2 hours, treated with 1μM S1P for 1 hour, fixed, and stained. Arrowheads indicate reticular junctions. Scale bar = 10μm. **(B)** Data represent average number of reticular junctions per field ± S.E. of at least 7 fields per group for three blinded independent experiments. The number of reticular junctions per field was significantly higher in shANXA2-1 cells (Student's *t*-test, ∗∗∗ $p<0.0001$).

To determine if we could recapitulate the formation of reticular junctions in ECs on coverslips, we first tested for optimal conditions for 48 hours of culture. ECs in culture were predicted to require serum to provide them with growth and survival signals; however, to determine the effects of S1P or other proangiogenic stimuli, placing ECs in low-serum medium would ensure cell quiescence. Therefore, to establish a low serum environment that maintains cell viability, confluent EC monolayers were seeded on collagen I-coated glass coverslips for 18 hours in growth medium (13% FBS). After 18 hours, the full serum medium was removed, the cells were rinsed three times with M199 and low serum medium ranging from 0.65% serum to 6.5% serum was added to the cells. After 48 hours in less than 2.6% serum, ECs detached from coverslips, indicating they were no longer healthy (Figure 13). Serum levels ranging from 6.5 to 2.6% serum promoted EC attachment and maintained a continuous monolayer. Therefore, all subsequent experiments used medium containing 2.6% serum to culture ECs on coverslips for longer than 24 hours.

The original report of reticular junctions by Millan and colleagues utilized fibronectin as a substrate (109). To test whether fibronectin is required for reticular junction formation, we seeded HUVECs onto glass coverslips coated with fibronectin, collagen type I, collagen IV, and Matrigel for 48 hours under quiescent, low serum (2.6%) conditions. Interestingly, we discovered the presence of reticular junctions on all matrix proteins tested (Figure 14). This observation led us to characterize the formation of these reticular junctions temporally.

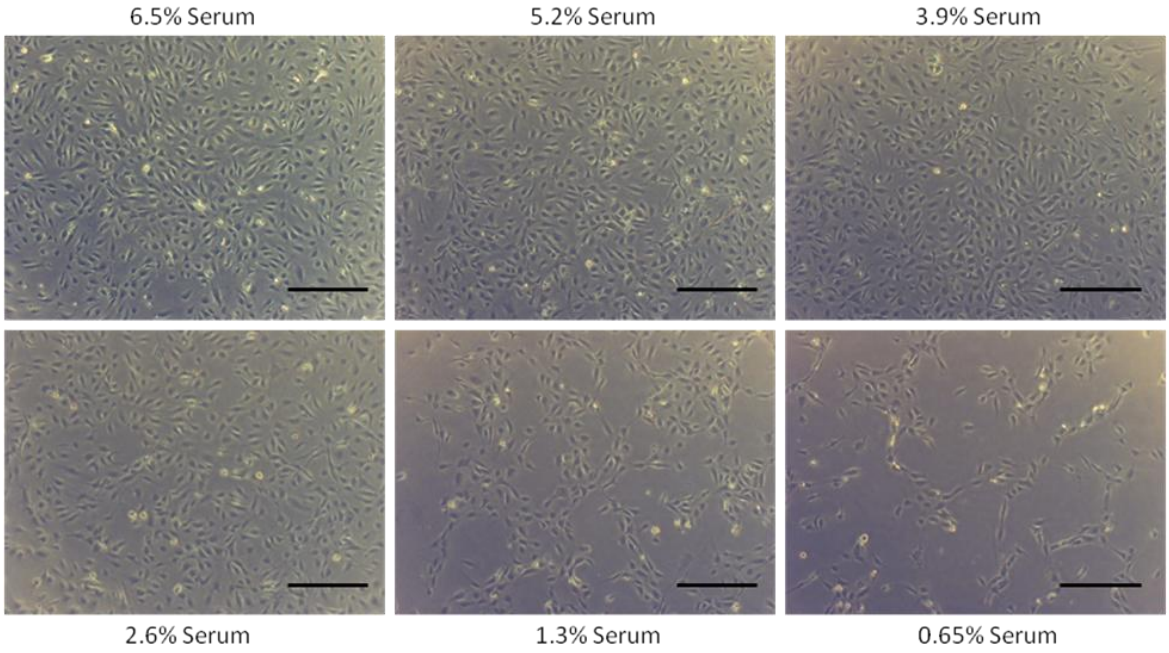

Figure 13. Establishing quiescent EC monolayers on 2D coverslips.
Representative phase images illustrating the cobblestone morphology and relative confluence of ECs when cultured under low serum conditions. HUVECs were seeded onto collagen I-coated glass coverslips and allowed to attach in media containing 13% fetal bovine serum overnight. After 18 hours the media was replaced with reduced-serum media; upper panels from left to right, cells in medium containing 6.5% serum, 5.2% serum, 3.9% serum; lower panels from left to right cells in medium containing 2.6% serum, 1.3% serum, and 0.65% serum. Cells were imaged after incubation for 48 hours. Scale bar = 100μm.

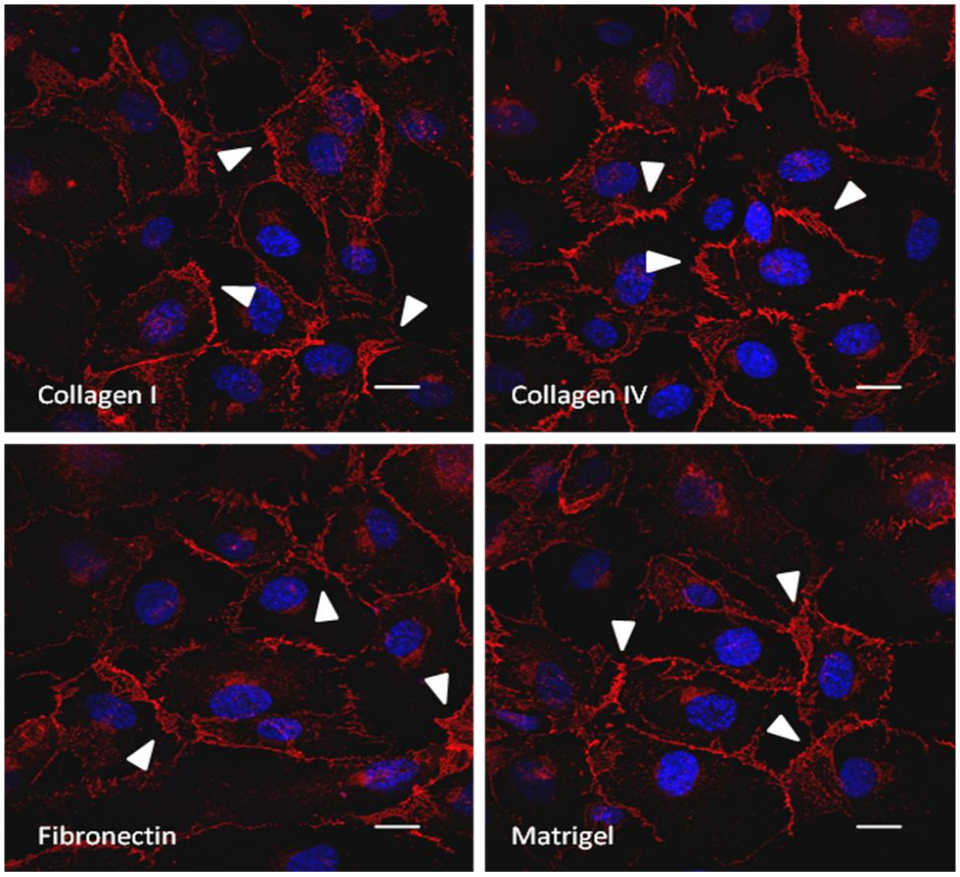

Figure 14. Reticular junctions form in ECs seeded on multiple matrix proteins under quiescent conditions.
Representative confocal EDF images illustrating the presence of reticular junctions in ECs seeded onto several matrix proteins under low serum conditions. ECs were seeded onto glass coverslips coated with 20µg/mL collagen I, collagen IV, fibronectin, and Matrigel. The cells were allowed to attach in media containing full serum (13%) overnight. After 18 hours the media was replaced with reduced-serum media (2.6%) for an additional 20 hours. The cells were then fixed and stained with VE-cadherin and imaged as shown in Figure 3. Nuclei are stained with 1µM DAPI (blue). Arrowheads indicate reticular junctions. Scale bar = 10µm.

HUVECs were seeded onto collagen I-coated coverslips and allowed to attach overnight in growth medium. After 18 hours the cells were placed in low serum (2.6% FBS) medium for indicated time ranging from 15 minutes to 12 hours before fixation, permeabilization, blocking, and staining. Figure 14A shows representative images of ECs stained with VE-cadherin and appropriate secondary antibodies conjugated to Alexa 594 from one of two independent experiments. After 15 minutes almost no reticular junctions are seen; however the number of reticular junctions identified per image increased with time (Figure 15A, B). There was a significant increase in the number of reticular junctions after 8 hours in culture on coverslips. Serum contains ~600nM S1P (120); as the cells are cultured in low serum, we suspect over time they undergo S1P withdrawal. This raises the possibility that the ECs create reticular junctions in response to S1P withdrawal. We also observed an increase in the relative amount of VE-cadherin after 4 hours (Figure 15C).

In addition to VE-cadherin expression, ZO-1 expression levels also changed over time. Figure 16A shows representative images of cells on coverslips prepared at time points ranging from 15 minutes to 12 hours as in Figure 15. The cells were stained with antibodies directed to ZO-1 and appropriate secondary antibodies conjugated to Alexa 488. The relative intensity levels of ZO-1 increased over time, Figure 16B. Compared to all earlier time points, the relative intensity of ZO-1 was significantly higher 12 hours after culture in low serum. If we compare this timeline to EC sprouting in 3D collagen matrices, sprout formation begins at approximately 3 hours and progresses to full cell invasion after 12 hours (112). It is tempting to speculate that VE-cadherin, ZO-1, and

reticular junctions may promote EC sprouting and invasion after 4 hours. Time course studies are underway to determine whether the formation of reticular junctions coincides with initiation of EC invasion into 3D collagen matrices.

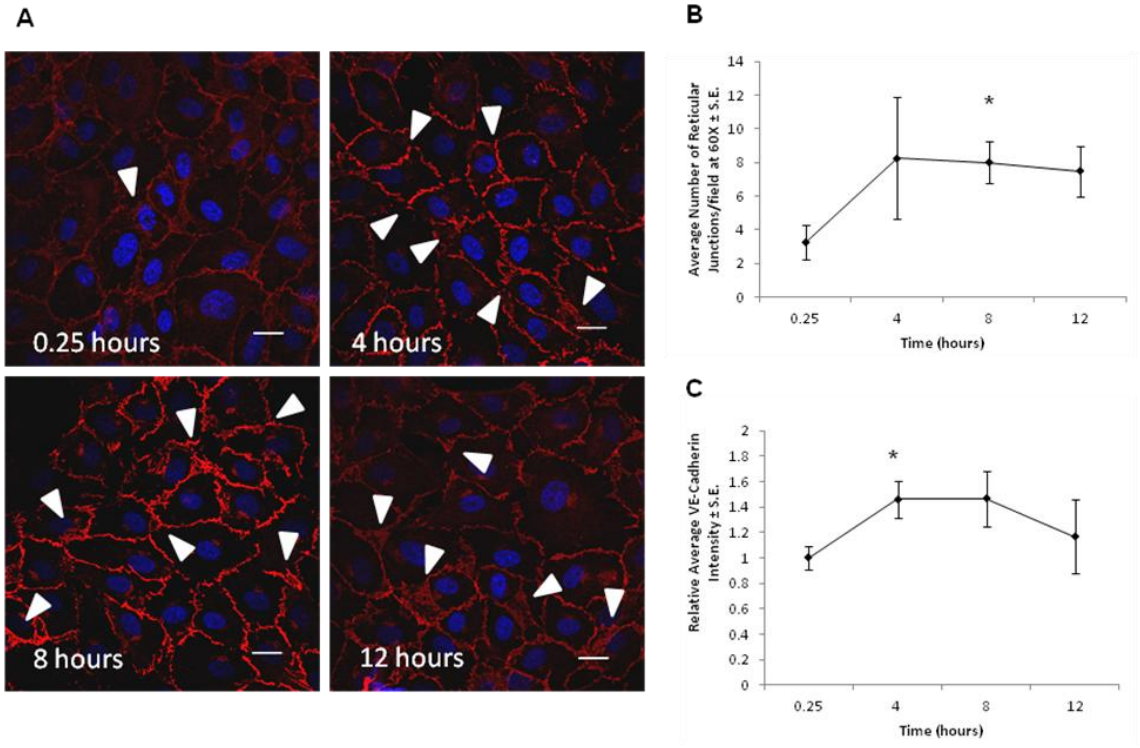

Figure 15. Reticular junction formation is time dependent.
(A) Representative confocal EDF images illustrating the presence of reticular junctions in ECs seeded onto glass coverslips coated with 20µg/mL of collagen I. The cells were allowed to attach in media containing full serum (13%) overnight. After 18 hours the media was replaced with reduced-serum media (2.6%) for an additional 0.25, 4, 8 or 12 hours. The cells were then fixed, and stained with VE-cadherin and imaged as shown in Figure 3. Nuclei were stained with 1µM DAPI (blue). Arrowheads indicate reticular junctions. Scale bar = 10µm. **(B)** Quantification of the number of reticular junctions observed with time. Two images were analyzed at each time point for two independent experiments. Data are presented as average number of reticular junctions per field ± S.E. using a 60× objective. There were significantly more reticular junctions after 8 hours in culture than after 0.25 hours. (Student's *t*-test, ∗ $p<0.05$). **(C)** Data are presented as the mean fluorescence intensity per field ± S.E. using a 60× objective and measured from EDF confocal images (2 images per group per experiment) using NIS Elements software and normalized to 0.25 hour time point. There was significantly more VE-cadherin after 4 hours in culture than after 0.25 hours. (Student's *t*-test, ∗ $p<0.05$).

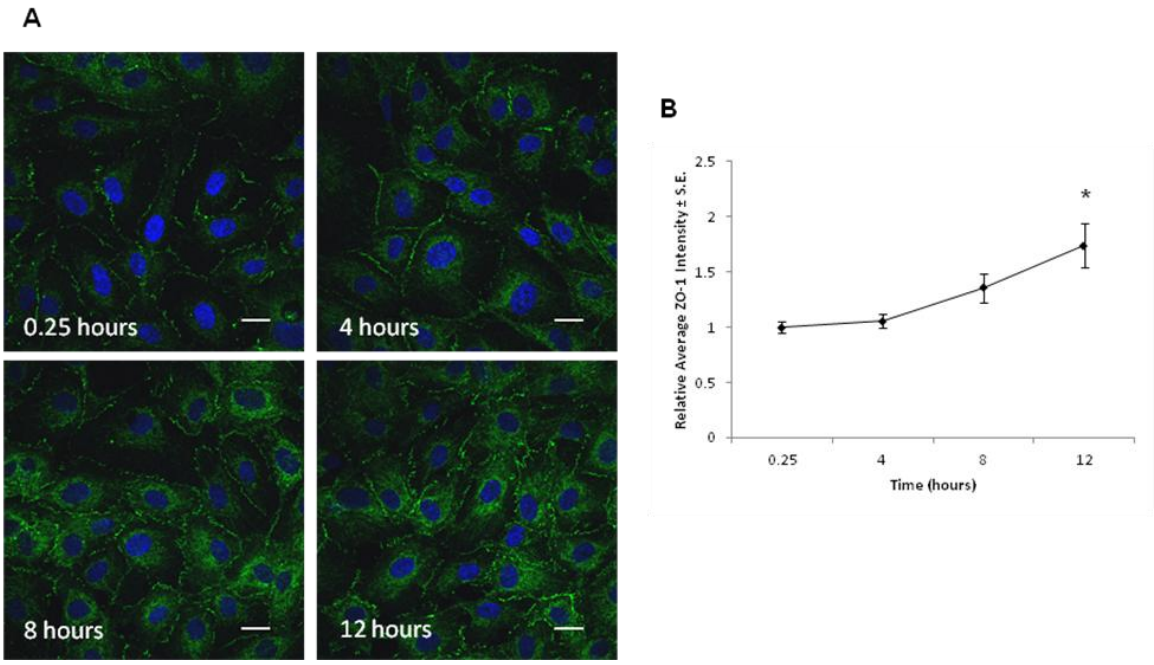

Figure 16. ZO-1 expression increases with time in reduced-serum medium.
(A) Representative confocal images from one of two independent experiments illustrating that ZO-1 expression increased with time. ECs were seeded on collagen I-coated glass coverslips overnight. After 18 hours cells were placed in low serum (2.6%) medium for 0.25, 4, 8, and 12 hours. Cells were then fixed and stained with primary antibodies directed to ZO-1 and secondary antibodies conjugated to Alexa 488. Nuclei were stained with 1μM DAPI (blue). Scale bar = 10μm. **(B)** Data are presented as the mean fluorescence intensity per field ± S.E. using a 60× objective and measured from EDF confocal images (2 images per group per experiment) using NIS Elements software and normalized to 0.25 hour time point. There was a significant increase in the relative intensity of ZO-1 after 12 hours in low serum culture when compared to the intensity after 15 minutes in low serum culture. (Student's *t*-test, ∗ $p<0.05$).

One interesting question raised by these results is whether a similar mechanism is responsible for formation of reticular junctions in response to both serum withdrawal, which is potentially due to lowering S1P levels, and the silencing of ANXA2 in ECs. These two types of reticular junctions are formed under different conditions; in particular, shANXA2-1 cells form reticular structures in the presence of S1P, while non-transduced ECs form reticular structures after 8 or more hours in low (2.6%) serum culture. In Figure 16, we tested whether non-transduced ECs would form reticular structures in the presence of S1P. Experiments were conducted as in Figures 15 and 16 with a single addition of 1μM S1P at time 0. The addition of S1P inhibited reticular junction formation throughout the 12 hours in culture (Figure 17A, B) suggesting S1P somehow prevented or opposed reticular junction formation. These data also raise the interesting possibility that serum withdrawal and loss of S1P signaling allows reticular junction formation. There were no significant differences in reticular junction formation between any of time points collected in the S1P treatment group (Figure 17B). However, there was a significant difference in the average number of reticular junctions at 8 hours between the No Treatment and S1P treatment groups. We are currently conducting experiments exploring the effect of FTY720 treatment, an S1P1 inhibitor (121), on the formation of reticular junctions. We expect these data will confirm whether antagonizing S1P signaling leads to the formation of reticular junctions.

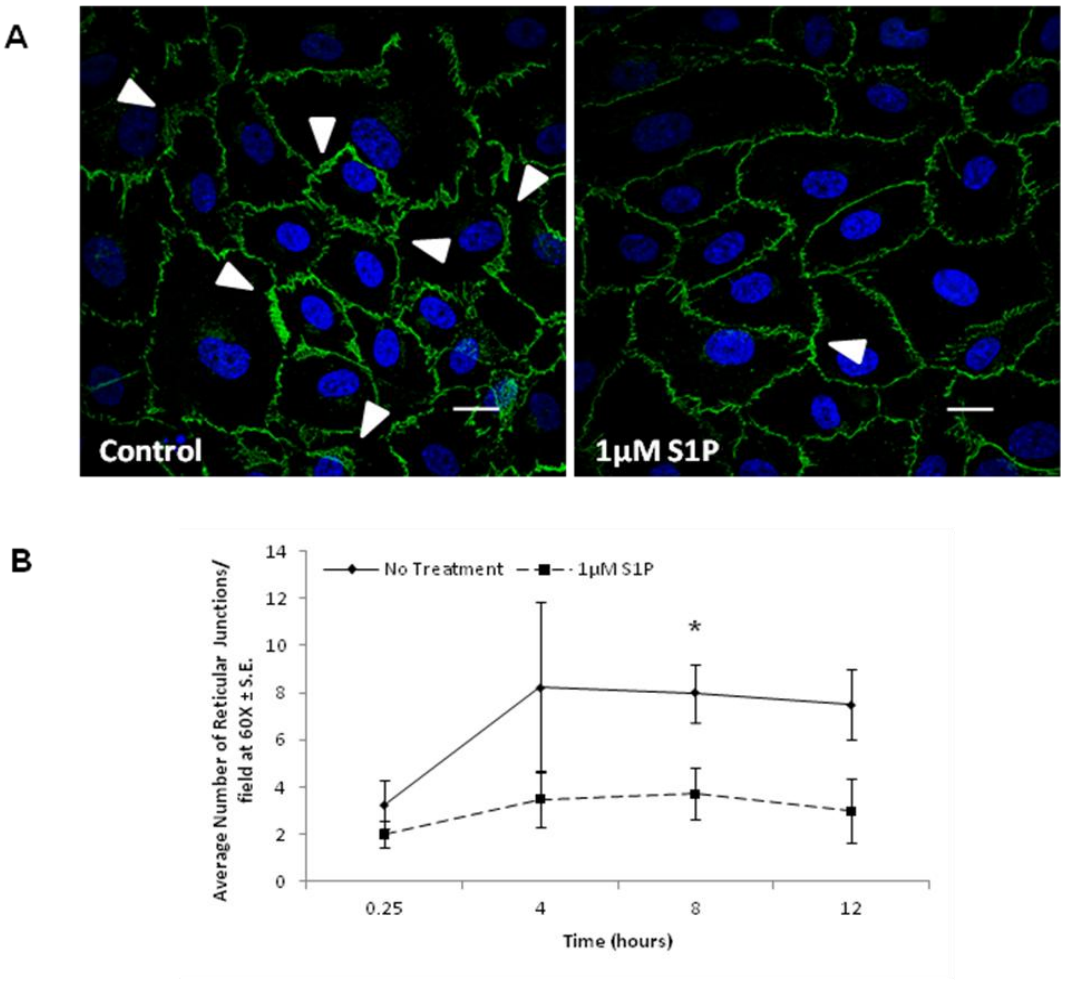

Figure 17. Reticular junction formation is inhibited by S1P.
(A) Representative confocal EDF images illustrating the presence of reticular junctions in ECs seeded onto glass coverslips coated with 20µg/mL of collagen I. The cells were allowed to attach in media containing full serum (13%) overnight. After 18 hours the media was replaced with reduced-serum media (2.6%) with either no treatment (control) or 1µM S1P for an additional 12 hours. The cells were then fixed, and stained with VE-cadherin primary antibodies and secondary antibodies conjugated to Alexa 488. Nuclei were stained with 1µM DAPI (blue). Arrowheads indicate reticular junctions. Scale bar = 10µm. **(B)** Quantification of the number of reticular junctions observed per field with time when ECs were placed in low serum for 12 hours with and without S1P treatment. Two images were collected and analyzed at each time point for each of two independent experiments. Data are presented as average number of reticular junctions per field using a 60× objective ± S.E. There were significantly less reticular junctions after 8 hours in culture with S1P treatment than in control group. Additionally, there was no significant increase in number of reticular junctions between timepoints with the addition of S1P as there was after 8 hours without S1P. (Student's *t*-test, ∗ $p<0.05$).

S1P appears to be a key factor in suppressing the formation of reticular junctions in non-transduced ECs; however, shANXA2 cells form reticular junctions despite the addition of S1P (Figure 11). To determine if the non-transduced reticular junctions have a similar protein distribution as the shANXA2 reticular junctions, we conducting co-staining experiments. Non-transduced HUVECs were seeded onto collagen I-coated coverslips and allowed to attach overnight in full serum. After 18 hours the cells were placed in low serum (2.6%) media for 12 hours with no treatment or with 1μM S1P before fixation, permeabilization, blocking and staining. ECs were co-stained with VE-cadherin and ZO-1 (Figure 18A), as well as VE-cadherin and paxillin (Figure 18B), and appropriate secondary antibodies conjugated to Alexa 488 and 594 from one of two independent experiments.

Ultimately, similar to the shANXA2 reticular junctions, the non-transduced EC reticular junctions exhibit no colocalization of VE-cadherin and ZO-1 or paxillin denoted by dotted circles, while the linear regions denoted by arrows show colocalization of VE-cadherin with either ZO-1 or paxillin. Also noteworthy is the relative size of the reticular junctions. 1μM S1P was added to stimulate paxillin movement to the linear junctions; however, reticular junction formation is opposed by S1P explaining the relatively small reticular junction in the S1P images compared to the cells not treated with S1P. Overall, despite the size difference with the addition of S1P, the protein localization in the non-transduced EC reticular junctions and the shANXA2 reticular junctions is similar.

Figure 18. Reticular junctions in non-transduced ECs have some similar attributes to reticular junctions formed in shANXA2 cells.
Representative confocal EDF images illustrating co-stains of non-transduced ECs that create reticular junctions similar to shANXA2 cells as seen in Figure 11. ECs were seeded on collagen I-coated glass coverslips overnight in growth medium containing 13% FBS. After 18 hours cells were placed in low serum (2.6%) medium for 12 hours either with no treatment or 1μM S1P, fixed, and stained with primary antibodies directed to **(A)** ZO-1 and VE-cadherin and corresponding secondary antibodies conjugated to Alexa 488 and 594, respectively or **(B)** VE-cadherin and paxillin and corresponding secondary antibodies conjugated to Alexa 488 and 594, respectively. ZO-1 does not colocalize with VE-cadherin at the reticular junction as in the No Treatment group, dotted circle; however, at linear junctions as seen with S1P treatment, ZO-1 and VE-cadherin colocalize. VE-cadherin and paxillin overlap with addition of S1P at linear junctions, arrow; however, as in the shANXA2 cells, paxillin did not localize with VE-cadherin at reticular junctions, dotted circle. Nuclei were stained with 1μM DAPI (blue). Scale bar = 5μm.

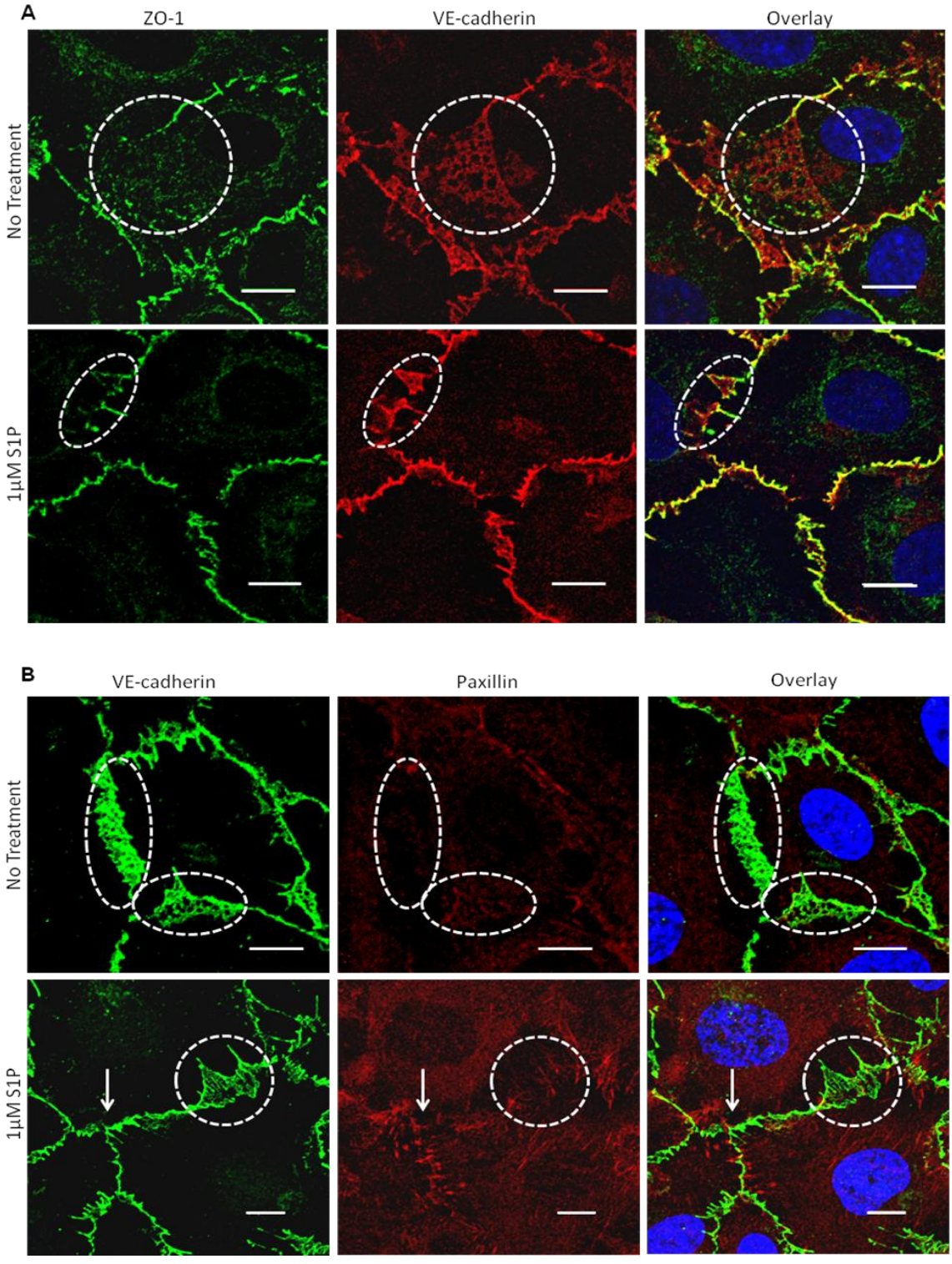
A
ZO-1
VE-cadherin
Overlay
No Treatment
1μM S1P
B
VE-cadherin
Paxillin
Overlay
No Treatment
1μM S1P

Because shANXA2 cells displayed an increase in the amount of reticular junctions and ANXA2 was required for EC sprouting in 3D collagen matrices (108), we tested whether reticular junctions were present in non-transduced EC monolayers during sprouting. HUVECs were seeded onto 3D collagen matrices (1mg/mL) containing 1μM S1P and 40ng/mL of VEGF and bFGF as previously described (112). After 24 hours samples containing invading cells were probed for ZO-1 and VE-cadherin using confocal microscopy. Analysis of the EC monolayer on the surface of the collagen matrices revealed the presence of numerous reticular junctions, as well as the presence of sprouts initiating from reticular junctions (Figure 19). The orientation of the images in the upper panels is a top down view where the arrow points to the open lumen of a newly formed sprout. The middle panels and lower panels display the same field in a 3D view at a 45^{o} angle and a side view, respectively. Noteworthy, are the number of cells and junctions involved in the sprout initiation shown confirming the importance of junctions during sprouting angiogenesis. These data suggest that reticular junctions may have a direct role in promoting EC sprouting.

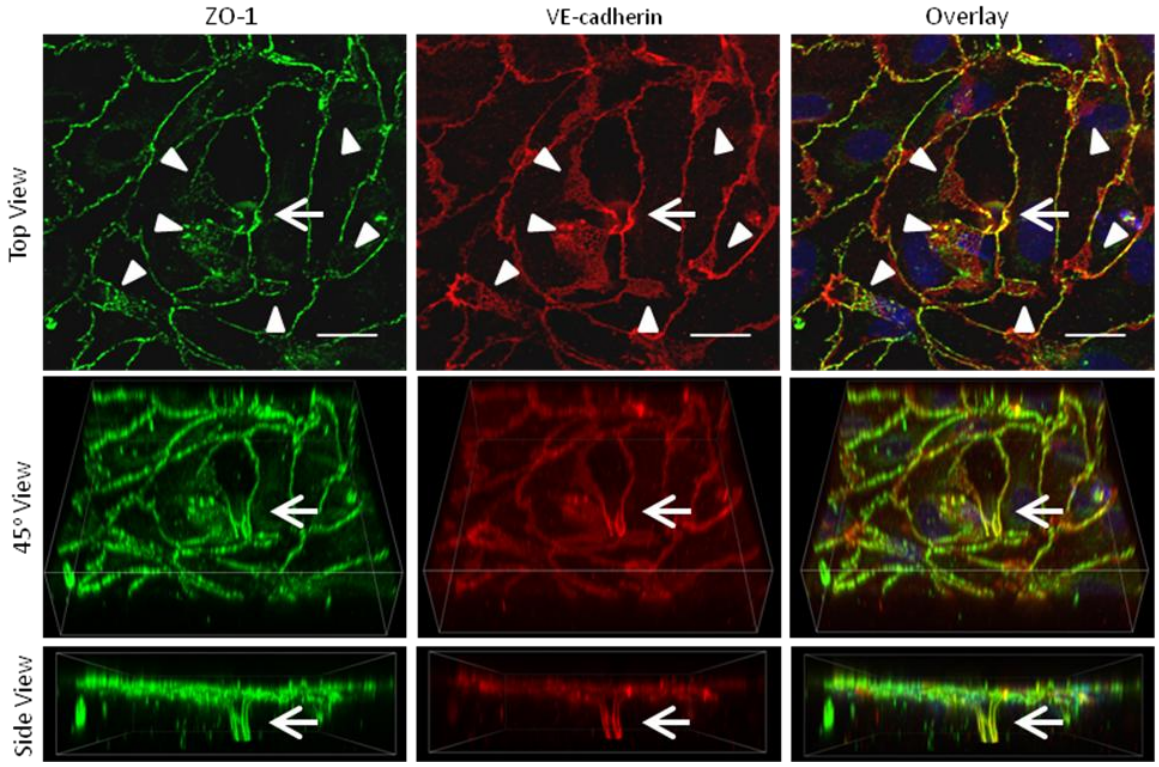

Figure 19. Invading sprouts initiate from reticular junctions in 3D.
Representative confocal EDF and 3D images illustrating sprout initiation from reticular junctions. Non-transduced ECs were seeded on 3D 1mg/mL collagen I matrices containing 1μM S1P and fed with low serum media containing 40ng/mL of VEGF and bFGF overnight. After 24 hours cells were fixed and stained with primary antibodies directed to ZO-1 and VE-cadherin and corresponding secondary antibodies conjugated to Alexa 488 and 594, respectively. Nuclei were stained with 1μM DAPI (blue). Upper panels display EDF images at a top down view. The middle panels display a view at a 45^{o} angle and the lower panels display a side view. Arrowheads indicate reticular junctions. Arrow indicates sprout initiation from reticular junctions. Scale bar = 10μm.

For all experiments shown, prior to this 3D experiment, ECs were cultured on glass coverslips coated with a thin layer of matrix proteins. Notably, 3D invasion experiments are conducted on collagen matrices, which are much more pliable. We suspect that changing the matrix stiffness or changing the concentration of the matrix proteins will affect the size or number of reticular junctions. Figure 20 shows representative images from a pilot study in which we compare the number of reticular junctions in non-transduced ECs seeded onto either 1mg/mL or 5mg/mL 3D collagen matrices. The experiment was conducted for 24 hours as in Figure 19 with S1P and growth factor treatment. This experiment will need to be repeated prior to quantification; however, at present it appears that ECs seeded on 5mg/mL gels form more reticular junctions than on 1mg/mL gels. Cells on 5mg/mL gels have an increased number of invading cells than cells on 1mg/mL gels (data not shown). Thus, the increased formation of reticular junctions on 5mg/mL gels, appears to correlate with a higher number of invading structures when compared to 1mg/mL gels. The location of the reticular junctions is also interesting. There are areas of natural alignment of the ECs. These areas contain many linear junctions and few reticular junctions; however, in the areas where the cells are not aligned, we notice more reticular junctions and fewer linear junctions suggesting cell misalignment may also contribute to reticular junction formation.

Finally, we used a mouse decidua model to determine the prevalence of reticular junctions *in vivo*. Following implantation, the maternal mouse uterine tissue undergoes a rapid transformation characterized by a robust angiogenic response. In Figure 21, we

observed blood vessels in the decidua surrounding the implantation site. In larger and more stabilized vessels, we observed EC alignment and linear EC junctions. In somewhat smaller and more tortuous vessels, presumably, vessels undergoing angiogenesis, the EC junctions, as illustrated by PECAM-1 staining, contain reticular regions. These data support the role of alignment in reticular junction formation and the presence of reticular junctions in vivo in tissue regions experiencing vascularization.

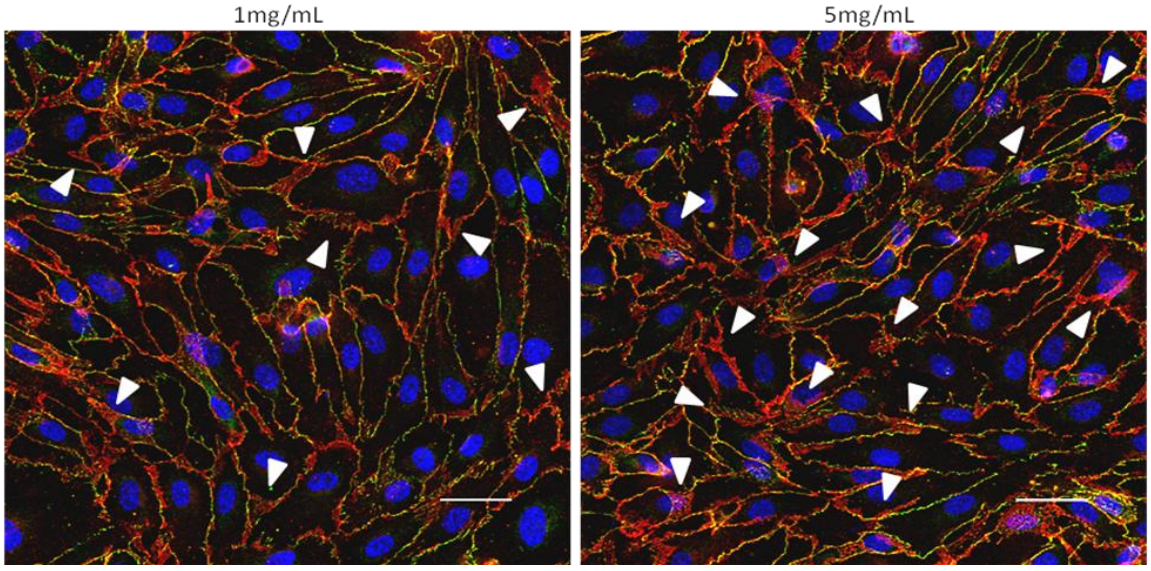

Figure 20. Increased collagen density increases number of reticular junctions in 3D. Representative confocal EDF images illustrating reticular junctions on 3D in 1 and 5mg/mL collagen I gels. Non-transduced ECs were seeded on 3D 1mg/mL or 5mg/mL collagen I matrices containing 1μM S1P and fed with low serum media containing 40ng/mL of VEGF and bFGF overnight. After 24 hours cells were fixed and stained with primary antibodies directed to ZO-1 and VE-cadherin and corresponding secondary antibodies conjugated to Alexa 488 and 594, respectively. Nuclei were stained with 1μM DAPI (blue). Data presented are representative of one independent experiment. Arrowheads indicate reticular junctions. Scale bar = 10μm.

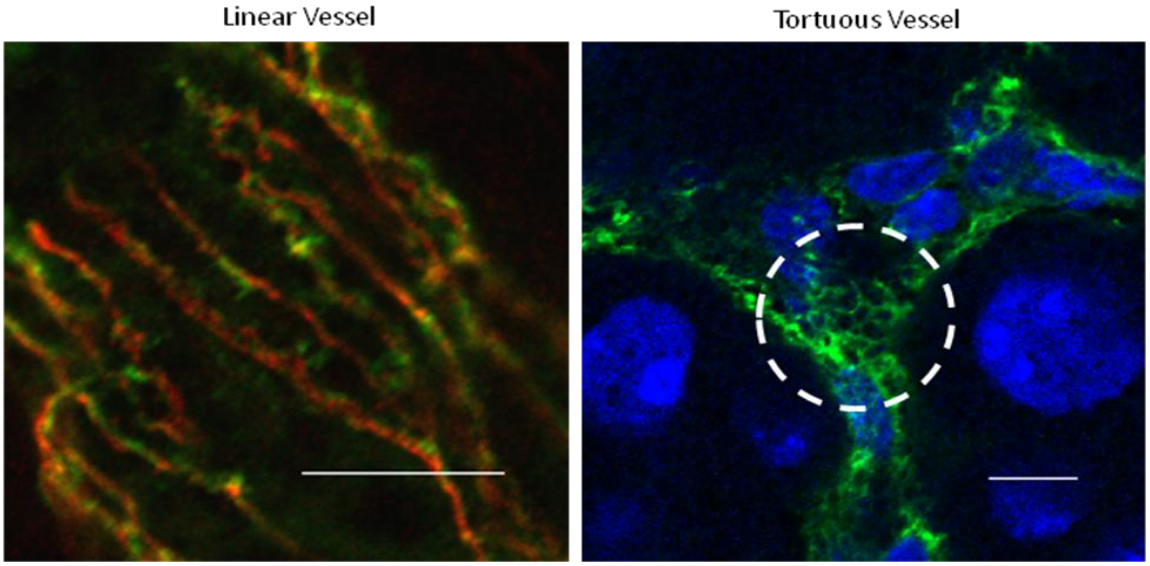

Figure 21. Reticular junctions present in tortuous vessels of mouse deciduas. Representative confocal EDF images illustrating reticular junctions in tortuous vessels, but not linear vessels in mouse decidua. 7.5 days after implantation mouse decidua tissue was harvested, fixed, and stained with primary antibodies directed to PECAM-1 and α-catenin, and corresponding secondary antibodies conjugated to Alexa 488 and 594, respectively. The left panel displays a stabilized vessel containing aligned ECs and linear junctions. The right panel displays a tortuous vessel containing reticular junctions. Nuclei were stained with 1μM DAPI (blue). Data presented are representative of one independent experiment. Dotted circle indicates reticular junctions. Scale bar = 5μm.

CHAPTER IV

DISCUSSION

We report here the importance of ANXA2 in EC junctional integrity, and in particular as a required protein for transducing S1P stimulation into barrier enchancement. To determine the importance of ANXA2 in junctional stability, we first generated and characterized ECs with the ANXA2 protein silenced by directed shRNA. Protein and mRNA silencing was successful for each of the clones in both the ANXA2 groups and control (β2M) groups as determined by qtPCR and Western Blot. Additionally, the morphology and cell size of the knockdown cells was not significantly different from the non-transduced ECs.

Upon analysis of the cell-cell junctions a wide reticular pattern was discovered in the ANXA2 knockdown cells following S1P treatment, while the control cells had linear cell-cell junctions as displayed by VE-cadherin staining. This reticular staining pattern was true for many adherens junction proteins including VE-cadherin, PECAM-1, Filamin A, and α- and β-catenin. Following analysis of the adherens junctions proteins, we detailed the affect ANXA2 removal has on focal adhesion proteins. Garcia and colleagues have shown that in addition to stimulating adherens junctions protein localization to the cell-cell junctions, S1P also stimulates focal adhesion proteins, such as paxillin and FAK to localize to cell-cell junctions (57). We show that localization of vinculin, a protein with roles both as a focal adhesion protein and a junctional protein (118), to cell-cell junctions is also enhanced by S1P treatment; however, when ANXA2

is silenced, neither FAK, paxillin, nor vinculin form large focal adhesions near the cell-cell junctions, particularly, near the reticular cell-cell junctions. Finally, we discovered that a tight junction protein, ZO-1 was not a member of the reticular junctions. ZO-1, stimulated by S1P to bind to α-catenin and enhance tight junction formation (91), did not localize in the same reticular pattern as α-catenin in cells lacking ANXA2. These data spur further questions about the association of reticular junctions lacking ANXA2 with the actin cytoskeleton under the influence of S1P. ANXA2 is required for the formation of actin-rich tight junctions (106) and reticular junctions formed in non-transduced cells lack significant actin localization (109), so we expect that reticular junctions lacking ANXA2 will be deficient in actin even in the presence of S1P, which stimulates the formation of actin-rich tight junctions (92). Ongoing experiments include reconstitution of Akt in shANXA2 cells. Akt is downstream of ANXA2 in the S1P signaling pathway, and reconstitution of Akt in shANXA2 cells has been shown to recover the invasive capacity of the ECs on 3D collagen matrices (108). Once generated, the cells will be assessed via immunofluorescence in both 2D and 3D experiments. We will be looking specifically for the recovered presence of linear adherens junctions, as well as the localization of focal adhesion proteins and actin at the EC junctions.

The discovery of reticular junctions in shANXA2 cells stimulated our interest in reticular junctions found in non-transduced and non-stimulated ECs. After defining a protocol for culturing cells on coverslips under quiescent conditions for over 48 hours, we repeated and expanded on the experiment that first discovered reticular junctions (109). We found reticular junctions forming on several matrix protein substrates and an

increase in the number of reticular junctions over time. A potential cause in the change in number of reticular junctions over time could be due to the relative changes in adherens junction and tight junction proteins, specifically VE-cadherin and ZO-1 (Figure 22). Between 4 hours and 12 hours on coverslips in low serum, the cells exhibit a loss of VE-cadherin fluorescence intensity and an increase in ZO-1 intensity that correlates with an increase in reticular junctions. Ultimately, we plan on looking at VE-cadherin and ZO-1 expression levels over time in cells lacking shANXA2 to determine if the removal of ANXA2 alters the regulation of these proteins over time.

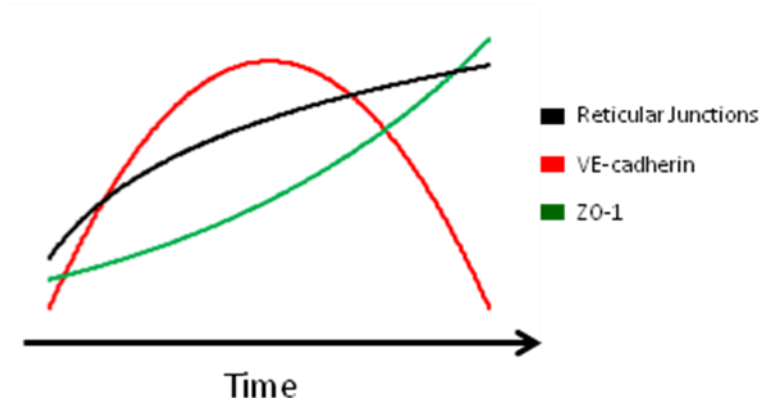

Figure 22. Schematic of trends in protein fluorescence and reticular junction prevalence.

The reticular junctions formed over time in non-transduced ECs resembled those formed in shANXA2 cells due to the consistent reticular localization of VE-cadherin, linear localization of ZO-1, and lack of paxillin at the reticular junctions in both groups. The primary difference between the two types of reticular junctions is their ability to respond to S1P treatment. shANXA2 cell junctions are reticular with the addition of S1P

and at early time points, where as non-transduced ECs do not form reticular junctions either at early time points or under the influence of S1P. In addition, qualitatively, the shANXA2 cell reticular junctions appear larger and much more developed than the non-transduced EC reticular junctions. Taken together, these data suggest that ANXA2 is required for a proper junctional response to S1P.

Interestingly, in 3D we discovered the presence of reticular junctions in non-transduced cells despite the presence of S1P. These data were unexpected due to our results in 2D illustrating a suppressive role of S1P in reticular junction formation. We speculate that the response to S1P is dependent on matrix stiffness and cell alignment. In 2D, on stiff glass, as the cells undergo S1P withdrawal, the ECs begin migrating onto each other in response to the stiff matrix to lessen the tension they sense causing reticular junctions to form. The addition of S1P fortifies the EC junctions in 2D as shown by (36) and enforces cell contact inhibition.

We also observed reticular junctions contributing to sprout initiation. The EC junctions are dynamic and able to change rapidly in response to proangiogenic stimuli. In Figure 23, we propose a model for the rapid reaction of ECs to S1P on 3D collagen matrices. Upon initial signaling, S1P causes an increase in the tight junction and adherens junction protein localization to the EC junctions in a linear pattern. Over time the activated cells begin to migrate on the soft substrate causing a reticular junction to form. We propose a tight junction remains intact on the apical side of the reticular junction. The cell will then begin to invade the soft matrix increasing its contact with the integrin binding sites in the matrix.

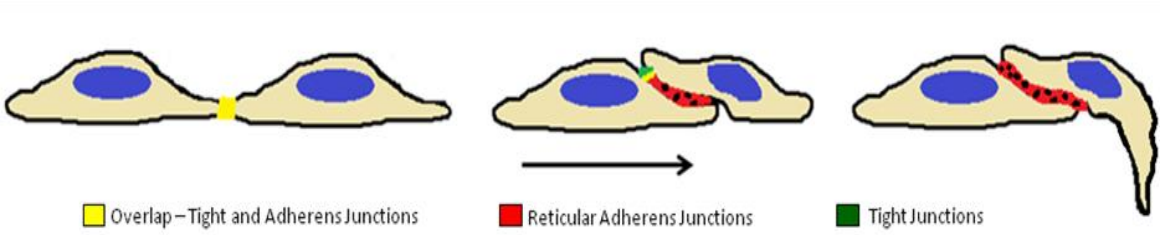

Figure 23. Proposed model for orientation of tight and reticular adherens junctions in sprouting ECs.

To confirm these speculations future studies will include the use of an S1P inhibitor in 2D to determine if reticular junctions increase over time. In addition, non-transduced ECs will be placed on 3D collagen gels to determine if reticular junction formation changes with time on 3D matrices in the presence of S1P. Another interesting experiment includes testing non-transduced ECs on collagen matrices without S1P to determine if S1P affects the ability of cells to create reticular junctions in 3D. To confirm data in Figure 20, cells will be seeded onto collagen matrices of differing collagen concentrations and reticular junctions will be quantified to determine if the matrix protein concentration affects reticular junction formation. Finally, we will continue to look in mouse uterine tissue samples at various stages of pregnancy when angiogenesis is abundant and characterize reticular junctions *in vivo*.

In summary, ANXA2 is required for EC junctional response to S1P, and is therefore required for EC sprout initiation as seen in our lab previously. Furthermore, this study provided insight into the dynamic nature of the endothelium and the EC junctions following activation by S1P, supporting a role for reticular junctions in sprouting angiogenesis.

CHAPTER V

CONLUSIONS

Removal of the ANXA2 protein in ECs results in the formation of wide reticular junctions in 2D, affecting localization of adherens junction proteins such as VE-cadherin, PECAM-1, filamin A, and α- and β-catenin. Focal adhesion proteins, such as paxillin and FAK, are stimulated to localize to adherens junctions by S1P (57). We show that vinculin localization to cell-cell junctions is also enhanced by S1P treatment; however, when ANXA2 is silenced, neither FAK, paxillin, nor vinculin form large focal adhesions near the cell-cell junctions, particularly, near the reticular cell-cell junctions.

Reticular junctions are reported in the literature in non-transduced cells seeded on fibronectin coated glass coverslips (109). We show that these reticular junctions are present in ECs seeded on collagen I-, collagen IV-, and Matrigel-coated glass coverslips in addition to fibronectin. We characterize these reticular junctions temporally, showing the number of reticular junctions increases over time, particularly after 8 hours in low serum culture medium. Levels of VE-cadherin and ZO-1 are also regulated over time in cells forming reticular junctions, upregulated at 4 hours and 12 hours, respectively. Most striking is the affect S1P has on reticular junction formation. The addition of S1P to ECs abrogates the formation of reticular junctions in 2D.

Upon comparison of the proteins involved, the shANXA2 reticular junctions and the non-transduced EC reticular junctions appear similar. In both groups only adherens junctions proteins participate in reticular localization while focal adhesion proteins and

tight junction proteins do not localize in a reticular pattern. The junctions differ, however, in that the shANXA2 reticular junctions form in the presence of S1P while the non-transduced reticular junctions do not, indicating ANXA2 is required for proper junctional response to S1P.

Finally, we show the presence of reticular junctions in EC monolayers on 3D collagen matrices, reticular junctions contributing to EC sprout initiation, and reticular junctions present in tortuous vessels *in vivo*. The discoveries detailed in this thesis illustrate the importance of ANXA2 in EC junctional response to S1P as well as the potential for future discoveries concerning the role of reticular junctions in sprouting angiogenesis.

REFERENCES

1. Risau W, Flamme I. 1995. Vasculogenesis. *Annual Review of Cell and Developmental Biology* 11:73-91
2. Ferguson JE, Kelley RW, Patterson C. 2005. Mechanisms of Endothelial Differentiation in Embryonic Vasculogenesis. *Arteriosclerosis, Thrombosis, and Vascular Biology* 25:2246-54
3. Gianni-Barrera R, Trani M, Fontanellaz C, Heberer M, Djonov V, et al. VEGF over-expression in skeletal muscle induces angiogenesis by intussusception rather than sprouting. *Angiogenesis* 16:123-36
4. Kim M, Park HJ, Seol JW, Jang JY, Cho Y-S, et al. 2013. VEGF-A regulated by progesterone governs uterine angiogenesis and vascular remodelling during pregnancy. *EMBO Molecular Medicine* 5:1415-30
5. Ribatti D, Djonov V. 2012. Intussusceptive microvascular growth in tumors. *Cancer Letters* 316:126-31
6. Carmeliet P, Jain RK. 2011. Molecular mechanisms and clinical applications of angiogenesis. *Nature* 473:298-307
7. Chung AS, Ferrara N. 2011. Developmental and pathological angiogenesis. *Annual Review of Cell and Developmental Biology* 27:563-84
8. Folkman J, D'Amore PA. 1996. Blood vessel formation: what is its molecular basis? *Cell* 87:1153-5
9. Carmeliet P. 2003. Angiogenesis in health and disease. *Nat Med* 9:653-60

10. Distler JH, Hirth A, Kurowska-Stolarska M, Gay RE, Gay S, Distler O. 2003. Angiogenic and angiostatic factors in the molecular control of angiogenesis. *The Quarterly Journal of Nuclear Medicine : Official Publication of the Italian Association of Nuclear Medicine (AIMN) [and] the International Association of Radiopharmacology (IAR)* 47:149-61

11. Kaunas R, Kang H, Bayless KJ. 2011. Synergistic Regulation of Angiogenic Sprouting by Biochemical Factors and Wall Shear Stress. *Cellular and Molecular Bioengineering* 4:547-59

12. Ribatti D, Nico B, Crivellato E, Roccaro AM, Vacca A. 2007. The history of the angiogenic switch concept. *Leukemia* 21:44-52

13. Abbasi T, Garcia JG. 2013. Sphingolipids in lung endothelial biology and regulation of vascular integrity. *Handbook of Experimental Pharmacology*:201-26

14. Ribatti D. 2005. The crucial role of vascular permeability factor/vascular endothelial growth factor in angiogenesis: a historical review. *British Journal of Haematology* 128:303-9

15. Phng LK, Gerhardt H. 2009. Angiogenesis: A Team Effort Coordinated by Notch. *Developmental Cell* 16:196-208

16. Kwak HI, Kang H, Dave JM, Mendoza EA, Su SC, et al. 2012. Calpain-mediated vimentin cleavage occurs upstream of MT1-MMP membrane translocation to facilitate endothelial sprout initiation. *Angiogenesis* 15:287-303

17. Kang H, Kwak HI, Kaunas R, Bayless KJ. 2011. Fluid shear stress and sphingosine 1-phosphate activate calpain to promote membrane type 1 matrix metalloproteinase (MT1-MMP) membrane translocation and endothelial invasion into three-dimensional collagen matrices. *The Journal of Biological Chemistry* 286:42017-26

18. Lee PF, Yeh AT, Bayless KJ. 2009. Nonlinear optical microscopy reveals invading endothelial cells anisotropically alter three-dimensional collagen matrices. *Experimental Cell Research* 315:396-410

19. van Hinsbergh VW, Koolwijk P. 2008. Endothelial sprouting and angiogenesis: matrix metalloproteinases in the lead. *Cardiovascular Research* 78:203-12

20. Stratman AN, Saunders WB, Sacharidou A, Koh W, Fisher KE, et al. 2009. Endothelial cell lumen and vascular guidance tunnel formation requires MT1-MMP-dependent proteolysis in 3-dimensional collagen matrices. *Blood* 114:237-47

21. Lammert E, Axnick J. 2012. Vascular lumen formation. *Cold Spring Harbor Perspectives in Medicine* 2:a006619

22. Stratman AN, Malotte KM, Mahan RD, Davis MJ, Davis GE. 2009. Pericyte recruitment during vasculogenic tube assembly stimulates endothelial basement membrane matrix formation. *Blood* 114:5091-101

23. Saez JC, Martinez AD, Branes MC, Gonzalez HE. 1998. Regulation of gap junctions by protein phosphorylation. *Braz J Med Biol Res* 31:593-600

24. Hossain MZ, Jagdale AB, Ao P, Boynton AL. 1999. Mitogen-activated protein kinase and phosphorylation of connexin43 are not sufficient for the disruption of gap junctional communication by platelet-derived growth factor and tetradecanoylphorbol acetate. *Journal of Cellular Physiology* 179:87-96

25. Hossain MZ, Jagdale AB, Ao P, Kazlauskas A, Boynton AL. 1999. Disruption of gap junctional communication by the platelet-derived growth factor is mediated via multiple signaling pathways. *The Journal of Biological Chemistry* 274:10489-96

26. Loewenstein WR, Rose B. 1992. The cell-cell channel in the control of growth. *Semin Cell Biol* 3:59-79

27. Esser S, Lampugnani MG, Corada M, Dejana E, Risau W. 1998. Vascular endothelial growth factor induces VE-cadherin tyrosine phosphorylation in endothelial cells. *Journal of Cell Science* 111:1853-65

28. Dejana E, Orsenigo F, Lampugnani MG. 2008. The role of adherens junctions and VE-cadherin in the control of vascular permeability. *Journal of Cell Science* 121:2115-22

29. Senger DR. 1983. Tumor Cells Secrete a Vascular-Permeability Factor that Promotes Accumulation of Ascites Fluid. *Science* 219:983-5

30. Folkman J. 1971. Tumor angiogenesis: therapeutic implications. *The New England Journal of Medicine* 285:1182-6

31. Montesano R, Pepper MS, Vassalli JD, Orci L. 1992. Modulation of angiogenesis in vitro. *Exs* 61:129-36

32. Aplin AC, Fogel E, Zorzi P, Nicosia RF. 2008. The aortic ring model of angiogenesis. *Methods in Enzymology* 443:119-36

33. Ando J, Kamiya A. 1993. Blood flow and vascular endothelial cell function. *Front Med Biol Eng* 5:245-64

34. Ichioka S, Shibata M, Kosaki K, Sato Y, Harii K, Kamiya A. 1997. Effects of shear stress on wound-healing angiogenesis in the rabbit ear chamber. *J Surg Res* 72:29-35

35. Hla T. 2004. Physiological and pathological actions of sphingosine 1-phosphate. *Seminars in Cell & Developmental Biology* 15:513-20

36. Lee M-J, Thangada S, Claffey KP, Ancellin N, Liu CH, et al. 1999. Vascular Endothelial Cell Adherens Junction Assembly and Morphogenesis Induced by Sphingosine-1-Phosphate. *Cell* 99:301-12

37. Dudek SM, Garcia JG. 2001. Cytoskeletal regulation of pulmonary vascular permeability. *Journal of Applied Physiology (Bethesda, Md. : 1985)* 91:1487-500

38. Schaphorst KL, Chiang E, Jacobs KN, Zaiman A, Natarajan V, et al. 2003. Role of sphingosine-1 phosphate in the enhancement of endothelial barrier integrity by platelet-released products. *American Journal of Physiology. Lung Cellular and Molecular Physiology* 285:L258-67

39. Garcia JG, Liu F, Verin AD, Birukova A, Dechert MA, et al. 2001. Sphingosine 1-phosphate promotes endothelial cell barrier integrity by Edg-dependent cytoskeletal rearrangement. *The Journal of Clinical Investigation* 108:689-701

40. Ryu Y, Takuwa N, Sugimoto N, Sakurada S, Usui S, et al. 2002. Sphingosine-1-phosphate, a platelet-derived lysophospholipid mediator, negatively regulates cellular Rac activity and cell migration in vascular smooth muscle cells. *Circ Res* 90:325-32

41. Kimura T, Watanabe T, Sato K, Kon J, Tomura H, et al. 2000. Sphingosine 1-phosphate stimulates proliferation and migration of human endothelial cells possibly through the lipid receptors, Edg-1 and Edg-3. *The Biochemical Journal* 348 Pt 1:71-6

42. Argraves KM, Wilkerson BA, Argraves WS. 2010. Sphingosine-1-phosphate signaling in vasculogenesis and angiogenesis. *World Journal of Biological Chemistry* 1:291-7

43. Vouret-Craviari V, Bourcier C, Boulter E, van Obberghen-Schilling E. 2002. Distinct signals via Rho GTPases and Src drive shape changes by thrombin and sphingosine-1-phosphate in endothelial cells. *J Cell Sci* 115:2475-84

44. Sabeh F, Li XY, Saunders TL, Rowe RG, Weiss SJ. 2009. Secreted versus membrane-anchored collagenases: relative roles in fibroblast-dependent collagenolysis and invasion. *The Journal of Biological Chemistry* 284:23001-11

45. Sato H, Takino T, Okada Y, Cao J, Shinagawa A, et al. 1994. A matrix metalloproteinase expressed on the surface of invasive tumour cells. *Nature* 370:61-5

46. Sun HY, Wei SP, Xu RC, Xu PX, Zhang WC. 2010. Sphingosine-1-phosphate induces human endothelial VEGF and MMP-2 production via transcription factor

ZNF580: novel insights into angiogenesis. *Biochem Biophys Res Commun* 395:361-6

47. Langlois S, Gingras D, Beliveau R. 2004. Membrane type 1-matrix metalloproteinase (MT1-MMP) cooperates with sphingosine 1-phosphate to induce endothelial cell migration and morphogenic differentiation. *Blood* 103:3020-8

48. Chun TH, Sabeh F, Ota I, Murphy H, McDonagh KT, et al. 2004. MT1-MMP-dependent neovessel formation within the confines of the three-dimensional extracellular matrix. *J Cell Biol* 167:757-67

49. Saunders WB, Bohnsack BL, Faske JB, Anthis NJ, Bayless KJ, et al. 2006. Coregulation of vascular tube stabilization by endothelial cell TIMP-2 and pericyte TIMP-3. *J Cell Biol* 175:179-91

50. Gingras D, Michaud M, Di Tomasso G, Beliveau E, Nyalendo C, Beliveau R. 2008. Sphingosine-1-phosphate induces the association of membrane-type 1 matrix metalloproteinase with p130Cas in endothelial cells. *FEBS letters* 582:399-404

51. Nyalendo C, Michaud M, Beaulieu E, Roghi C, Murphy G, et al. 2007. Src-dependent phosphorylation of membrane type I matrix metalloproteinase on cytoplasmic tyrosine 573: role in endothelial and tumor cell migration. *The Journal of Biological Chemistry* 282:15690-9

52. Li XY, Ota I, Yana I, Sabeh F, Weiss SJ. 2008. Molecular dissection of the structural machinery underlying the tissue-invasive activity of membrane type-1 matrix metalloproteinase. *Mol Biol Cell* 19:3221-33

53. Sato T, Iwai M, Sakai T, Sato H, Seiki M, et al. 1999. Enhancement of membrane-type 1-matrix metalloproteinase (MT1-MMP) production and sequential activation of progelatinase A on human squamous carcinoma cells co-cultured with human dermal fibroblasts. *British Journal of Cancer* 80:1137-43

54. Ancellin N, Hla T. 1999. Differential pharmacological properties and signal transduction of the sphingosine 1-phosphate receptors EDG-1, EDG-3, and EDG-5. *The Journal of Biological Chemistry* 274:18997-9002

55. Muraki K, Imaizumi Y. 2001. A novel function of sphingosine-1-phosphate to activate a non-selective cation channel in human endothelial cells. *The Journal of Physiology* 537:431-41

56. Mehta D, Konstantoulaki M, Ahmmed GU, Malik AB. 2005. Sphingosine 1-phosphate-induced mobilization of intracellular Ca2+ mediates rac activation and adherens junction assembly in endothelial cells. *The Journal of Biological Chemistry* 280:17320-8

57. Sun X, Shikata Y, Wang L, Ohmori K, Watanabe N, et al. 2009. Enhanced interaction between focal adhesion and adherens junction proteins: involvement in sphingosine 1-phosphate-induced endothelial barrier enhancement. *Microvasc Res* 77:304-13

58. Singleton PA, Dudek SM, Chiang ET, Garcia JG. 2005. Regulation of sphingosine 1-phosphate-induced endothelial cytoskeletal rearrangement and barrier enhancement by S1P1 receptor, PI3 kinase, Tiam1/Rac1, and alpha-actinin. *FASEB journal : Official Publication of the Federation of American Societies for Experimental Biology* 19:1646-56

59. Qi X, Okamoto Y, Murakawa T, Wang F, Oyama O, et al. 2010. Sustained delivery of sphingosine-1-phosphate using poly(lactic-co-glycolic acid)-based microparticles stimulates Akt/ERK-eNOS mediated angiogenesis and vascular maturation restoring blood flow in ischemic limbs of mice. *Eur J Pharmacol* 634:121-31

60. Bazzoni G, Dejana E. 2004. Endothelial Cell-to-Cell Junctions: Molecular Organization and Role in Vascular Homeostasis. *Physiological Reviews* 84:869-901

61. Simionescu M. 2000. Structural biochemical and functional differentiation of the vascular endothelium. . *Amsterdam: Harwood Academic*:1-20

62. Dejana E. 2004. Endothelial cell-cell junctions: happy together. *Nat Rev Mol Cell Biol* 5:261-70

63. Söhl G, Willecke K. 2004. Gap junctions and the connexin protein family. *Cardiovascular Research* 62:228-32

64. Ayalon O, Sabanai H, Lampugnani MG, Dejana E, Geiger B. 1994. Spatial and temporal relationships between cadherins and PECAM-1 in cell-cell junctions of human endothelial cells. *The Journal of Cell Biology* 126:247-58

65. Heimark RL, Degner M, Schwartz SM. 1990. Identification of a Ca2(+)-dependent cell-cell adhesion molecule in endothelial cells. *The Journal of Cell Biology* 110:1745-56

66. Sun QH, DeLisser HM, Zukowski MM, Paddock C, Albelda SM, Newman PJ. 1996. Individually distinct Ig homology domains in PECAM-1 regulate homophilic binding and modulate receptor affinity. *The Journal of Biological Chemistry* 271:11090-8

67. Albelda SM, Oliver PD, Romer LH, Buck CA. 1990. EndoCAM: a novel endothelial cell-cell adhesion molecule. *The Journal of Cell Biology* 110:1227-37

68. Carmeliet P, Lampugnani MG, Moons L, Breviario F, Compernolle V, et al. 1999. Targeted deficiency or cytosolic truncation of the VE-cadherin gene in mice impairs VEGF-mediated endothelial survival and angiogenesis. *Cell* 98:147-57

69. Provost E, Rimm DL. 1999. Controversies at the cytoplasmic face of the cadherin-based adhesion complex. *Curr Opin Cell Biol* 11:567-72

70. Wallez Y, Vilgrain I, Huber P. 2006. Angiogenesis: The VE-Cadherin Switch. *Trends in Cardiovascular Medicine* 16:55-9

71. Yamada S, Pokutta S, Drees F, Weis WI, Nelson WJ. 2005. Deconstructing the cadherin-catenin-actin complex. *Cell* 123:889-901

72. Kowalczyk AP, Navarro P, Dejana E, Bornslaeger EA, Green KJ, et al. 1998. VE-cadherin and desmoplakin are assembled into dermal microvascular endothelial intercellular junctions: a pivotal role for plakoglobin in the

recruitment of desmoplakin to intercellular junctions. *J Cell Sci* 111 (Pt 20):3045-57

73. Daniel JM, Reynolds AB. 1997. Tyrosine phosphorylation and cadherin/catenin function. *Bioessays* 19:883-91

74. Esser S, Lampugnani MG, Corada M, Dejana E, Risau W. 1998. Vascular endothelial growth factor induces VE-cadherin tyrosine phosphorylation in endothelial cells. *J Cell Sci* 111 (Pt 13):1853-65

75. Eichmann A, Simons M. 2012. VEGF signaling inside vascular endothelial cells and beyond. *Current Opinion in Cell Biology* 24:188-93

76. Koch S, Claesson-Welsh L. 2012. Signal Transduction by Vascular Endothelial Growth Factor Receptors. *Cold Spring Harbor Perspectives in Medicine* 2

77. DeLisser HM. 1997. Involvement of endothelial PECAM-1/CD31 in angiogenesis. *American Journal of Pathology* 151:671-7

78. Cao G, O'Brien CD, Zhou Z, Sanders SM, Greenbaum JN, et al. 2002. Involvement of human PECAM-1 in angiogenesis and in vitro endothelial cell migration. *American Journal of Physiology - Cell Physiology* 282:C1181-C90

79. Ilan N, Madri JA. 2003. PECAM-1: old friend, new partners. *Current Opinion in Cell Biology* 15:515-24

80. Osawa M, Masuda M, Kusano K, Fujiwara K. 2002. Evidence for a role of platelet endothelial cell adhesion molecule-1 in endothelial cell mechanosignal transduction: is it a mechanoresponsive molecule? *J Cell Biol* 158:773-85

81. Conway D, Schwartz MA. 2012. Lessons from the endothelial junctional mechanosensory complex. In *F1000 Biology Reports*

82. Tzima E, Irani-Tehrani M, Kiosses WB, Dejana E, Schultz DA, et al. 2005. A mechanosensory complex that mediates the endothelial cell response to fluid shear stress. *Nature* 437:426-31

83. Gratzinger D, Canosa S, Engelhardt B, Madri JA. 2003. Platelet endothelial cell adhesion molecule-1 modulates endothelial cell motility through the small G-protein Rho. *The FASEB Journal* 17:1458-69

84. Su S-C, Mendoza EA, Kwak H-i, Bayless KJ. 2008. Molecular profile of endothelial invasion of three-dimensional collagen matrices: insights into angiogenic sprout induction in wound healing. *American Journal of Physiology - Cell Physiology* 295:C1215-C29

85. Farquhar MG, Palade GE. 1963. Junctional complexes in various epithelia. *J Cell Biol* 17:375-412

86. Runkle EA, Mu D. 2013. Tight junction proteins: From barrier to tumorigenesis. *Cancer letters* 337:41-8

87. Stevenson BR, Siliciano JD, Mooseker MS, Goodenough DA. 1986. Identification of ZO-1: a high molecular weight polypeptide associated with the tight junction (zonula occludens) in a variety of epithelia. *The Journal of Cell Biology* 103:755-66

88. Harhaj NS, Antonetti DA. 2004. Regulation of tight junctions and loss of barrier function in pathophysiology. *The International Journal of Biochemistry & Cell Biology* 36:1206-37

89. Argaw AT, Gurfein BT, Zhang Y, Zameer A, John GR. 2009. VEGF-mediated disruption of endothelial CLN-5 promotes blood-brain barrier breakdown. *Proceedings of the National Academy of Sciences* 106:1977-82

90. Tsukita S, Furuse M. 2002. Claudin-based barrier in simple and stratified cellular sheets. *Current Opinion in Cell Biology* 14:531-6

91. Lee JF, Zeng Q, Ozaki H, Wang L, Hand AR, et al. 2006. Dual roles of tight junction-associated protein, zonula occludens-1, in sphingosine 1-phosphate-mediated endothelial chemotaxis and barrier integrity. *The Journal of Biological Chemistry* 281:29190-200

92. Dudek SM, Jacobson JR, Chiang ET, Birukov KG, Wang P, et al. 2004. Pulmonary endothelial cell barrier enhancement by sphingosine 1-phosphate: roles for cortactin and myosin light chain kinase. *The Journal of Biological Chemistry* 279:24692-700

93. Itoh M, Nagafuchi A, Moroi S, Tsukita S. 1997. Involvement of ZO-1 in cadherin-based cell adhesion through its direct binding to alpha catenin and actin filaments. *J Cell Biol* 138:181-92

94. Ikenouchi J, Umeda K, Tsukita S, Furuse M, Tsukita S. 2007. Requirement of ZO-1 for the formation of belt-like adherens junctions during epithelial cell polarization. *J Cell Biol* 176:779-86

95. Taddei A, Giampietro C, Conti A, Orsenigo F, Breviario F, et al. 2008. Endothelial adherens junctions control tight junctions by VE-cadherin-mediated upregulation of claudin-5. *Nat Cell Biol* 10:923-34

96. Giampietro C, Taddei A, Corada M, Sarra-Ferraris GM, Alcalay M, et al. 2012. Overlapping and divergent signaling pathways of N-cadherin and VE-cadherin in endothelial cells. *Blood* 119:2159-70

97. Burgering BM, Kops GJ. 2002. Cell cycle and death control: long live Forkheads. *Trends in Biochemical Sciences* 27:352-60

98. Brink PR, Cronin K, Banach K, Peterson E, Westphale EM, et al. 1997. Evidence for heteromeric gap junction channels formed from rat connexin43 and human connexin37. *Am J Physiol* 273:C1386-96

99. Bharadwaj A, Bydoun M, Holloway R, Waisman D. 2013. Annexin A2 heterotetramer: structure and function. *Int J Mol Sci* 14:6259-305

100. Madureira PA, Hill R, Miller VA, Giacomantonio C, Lee PW, Waisman DM. 2011. Annexin A2 is a novel cellular redox regulatory protein involved in tumorigenesis. *Oncotarget* 2:1075-93

101. Gou D, Mishra A, Weng T, Su L, Chintagari NR, et al. 2008. Annexin A2 interactions with Rab14 in alveolar type II cells. *The Journal of Biological Chemistry* 283:13156-64

102. Leoni G, Alam A, Neumann PA, Lambeth JD, Cheng G, et al. 2013. Annexin A1, formyl peptide receptor, and NOX1 orchestrate epithelial repair. *The Journal of Clinical Investigation* 123:443-54

103. Rankin CR, Hilgarth RS, Leoni G, Kwon M, Den Beste KA, et al. 2013. Annexin A2 regulates beta1 integrin internalization and intestinal epithelial cell migration. *The Journal of Biological Chemistry* 288:15229-39

104. Heyraud S, Jaquinod M, Durmort C, Dambroise E, Concord E, et al. 2008. Contribution of annexin 2 to the architecture of mature endothelial adherens junctions. *Molecular and Cellular Biology* 28:1657-68

105. Gerke V, Weber K. 1984. Identity of p36K phosphorylated upon Rous sarcoma virus transformation with a protein purified from brush borders; calcium-dependent binding to non-erythroid spectrin and F-actin. *The EMBO Journal* 3:227-33

106. Yamada A, Fujita N, Sato T, Okamoto R, Ooshio T, et al. 2006. Requirement of nectin, but not cadherin, for formation of claudin-based tight junctions in annexin II-knockdown MDCK cells. *Oncogene* 25:5085-102

107. Singleton PA, Mirzapoiazova T, Guo Y, Sammani S, Mambetsariev N, et al. 2010. High-molecular-weight hyaluronan is a novel inhibitor of pulmonary vascular leakiness. *American Journal of Physiology. Lung Cellular and Molecular Physiology* 299:L639-51

108. Su SC, Maxwell SA, Bayless KJ. 2010. Annexin 2 regulates endothelial morphogenesis by controlling AKT activation and junctional integrity. *The Journal of Biological Chemistry* 285:40624-34

109. Fernandez-Martin L, Marcos-Ramiro B, Bigarella CL, Graupera M, Cain RJ, et al. 2012. Crosstalk between reticular adherens junctions and platelet endothelial

cell adhesion molecule-1 regulates endothelial barrier function. *Arterioscler Thromb Vasc Biol* 32:e90-102

110. Cottrell GT, Burt JM. 2001. Heterotypic gap junction channel formation between heteromeric and homomeric Cx40 and Cx43 connexons. *Am J Physiol Cell Physiol* 281:C1559-67

111. Maciag T, Cerundolo J, Ilsley S, Kelley PR, Forand R. 1979. An endothelial cell growth factor from bovine hypothalamus: identification and partial characterization. *Proceedings of the National Academy of Sciences of the United States of America* 76:5674-8

112. Bayless K, Bayless H-I, Kwak S-C. 2009. Investigating endothelial invasion and sprouting behavior in three-dimensional collagen matrices. *Nature Protocols* 4:1888-98

113. Vinals F, Pouyssegur J. 1999. Confluence of vascular endothelial cells induces cell cycle exit by inhibiting p42/p44 mitogen-activated protein kinase activity. *Molecular and Cellular Biology* 19:2763-72

114. Fagotto F, Gumbiner BM. 1996. Cell Contact-Dependent Signaling. *Developmental Biology* 180:445-54

115. Lampugnani MG, Zanetti A, Breviario F, Balconi G, Orsenigo F, et al. 2002. VE-cadherin regulates endothelial actin activating Rac and increasing membrane association of Tiam. *Mol Biol Cell* 13:1175-89

116. Pece S, Gutkind JS. 2000. Signaling from E-cadherins to the MAPK pathway by the recruitment and activation of epidermal growth factor receptors upon cell-cell contact formation. *The Journal of Biological Chemistry* 275:41227-33

117. Pece S, Chiariello M, Murga C, Gutkind JS. 1999. Activation of the protein kinase Akt/PKB by the formation of E-cadherin-mediated cell-cell junctions. Evidence for the association of phosphatidylinositol 3-kinase with the E-cadherin adhesion complex. *The Journal of Biological Chemistry* 274:19347-51

118. Huveneers S, Oldenburg J, Spanjaard E, van der Krogt G, Grigoriev I, et al. 2012. Vinculin associates with endothelial VE-cadherin junctions to control force-dependent remodeling. *J Cell Biol* 196:641-52

119. Fraley SI, Feng Y, Krishnamurthy R, Kim D-H, Celedon A, et al. 2010. A distinctive role for focal adhesion proteins in three-dimensional cell motility. *Nat Cell Biol* 12:598-604

120. Hammad SM, Pierce JS, Soodavar F, Smith KJ, Al Gadban MM, et al. 2010. Blood sphingolipidomics in healthy humans: impact of sample collection methodology. *Journal of Lipid Research* 51:3074-87

121. Krump-Konvalinkova V, Chwalla I, Siess W. 2008. FTY720 inhibits S1P-mediated endothelial healing: relationship to S1P1-receptor surface expression. *Biochem Biophys Res Commun* 370:603-8